AD_____

Award Number: W81XWH-05-1-0427

TITLE: Unmasking Stem/Progenitor Cell Properties in Differentiated Epithelial Cells Using Short-term Transplantation

PRINCIPAL INVESTIGATOR: Michael T. Lewis

CONTRACTING ORGANIZATION: Baylor College of Medicine
Houston TX 77030

REPORT DATE: August 2006

TYPE OF REPORT: Annual

PREPARED FOR: U.S. Army Medical Research and Materiel Command
Fort Detrick, Maryland 21702-5012

REPORT DOCUMENTATION PAGE

Form Approved
OMB No. 0704-0188

1. REPORT DATE	2. REPORT TYPE	3. DATES COVERED
01-08-2006	Annual	20 Jul 2005 – 19 Jul 2006

4. TITLE AND SUBTITLE

Unmasking Stem/Progenitor Cell Properties in Differentiated Epithelial Cells Using Short-term Transplantation

5a. CONTRACT NUMBER

5b. GRANT NUMBER
W81XWH-05-1-0427

5c. PROGRAM ELEMENT NUMBER

6. AUTHOR(S)

Michael T. Lewis

E-Mail:

5d. PROJECT NUMBER

5e. TASK NUMBER

5f. WORK UNIT NUMBER

7. PERFORMING ORGANIZATION NAME(S) AND ADDRESS(ES)

Baylor College of Medicine
Houston TX 77030

8. PERFORMING ORGANIZATION REPORT NUMBER

9. SPONSORING / MONITORING AGENCY NAME(S) AND ADDRESS(ES)
U.S. Army Medical Research and Materiel Command
Fort Detrick, Maryland 21702-5012

10. SPONSOR/MONITOR'S ACRONYM(S)

11. SPONSOR/MONITOR'S REPORT NUMBER(S)

12. DISTRIBUTION / AVAILABILITY STATEMENT
Approved for Public Release; Distribution Unlimited

13. SUPPLEMENTARY NOTES
Original contains colored plates: ALL DTIC reproductions will be in black and white.

14. ABSTRACT

Background: Prevailing models maintain that stem cells comprise a minority of epithelial cells. However, some data suggest the percentage of mammary stem cells may be underestimated using common assays. **Rationale**: Short term transplantation using fragments of mammary duct offer an opportunity to test the prevailing stem cell model. If division-competent stem cells represent a small percentage of all epithelial cells, the initial rate of cell division in transplanted fragments should be low. However, if stem cells can include more differentiated, yet division-competent cells, the initial rate of cell division in fragments should be high **Objectives**: 1) To determine the range of mammary stem cell types participating in gland regeneration. 2) To develop the short-term transplantation assay as a means by which critical regulators of stem and progenitor cell behavior can be discovered and evaluated. **Relevance**: Studies will provide a direct test of prevailing stem cell models.

15. SUBJECT TERMS
Stem cells, mammary gland, transplantation

16. SECURITY CLASSIFICATION OF:			17. LIMITATION OF ABSTRACT	18. NUMBER OF PAGES	19a. NAME OF RESPONSIBLE PERSON
a. REPORT	b. ABSTRACT	c. THIS PAGE			USAMRMC
U	U	U	UU	47	19b. TELEPHONE NUMBER *(include area code)*

Table of Contents

Cover……1

SF 298……2

Introduction……4

Body……4

Key Research Accomplishments……8

Reportable Outcomes……9

Conclusions……9

References……10

Appendices……11

Introduction

Normal mammary epithelial stem cells are long-lived, self-renewing, and give rise to all progenitor and differentiated epithelial cell types. They are also hypothesized to be the cell of origin for breast cancer (Clarke et al., 2003). In breast cancer, it is thought that a sub-population of "cancer stem cells" having self-renewal and differentiation mechanisms similar to those of normal stem cells, might be resistant to common therapies, and therefore be responsible for treatment failure and disease recurrence. Thus, it is essential to define the full range of division-competent stem/progenitor cell types in the mammary gland and to understand their regulation for successful treatment of breast cancer.

Normal mammary stem cells are distributed throughout the ductal tree. Limiting dilution transplantation and *in vitro* "mammosphere" forming assays using dissociated epithelial cells suggest stem cells express CD29 and CD24 or CD49f and CD24 and represent about 1 in ~1,400 cells (Shackleton et al., 2006; Stingl et al., 2006). Coupled with electron microscopy (EM) studies showing only three division-competent epithelial cell types in the intact mouse mammary gland, these data support prevailing models in which division-competent stem/progenitor cells comprise only a minority of epithelial cells (Smith and Boulanger, 2003).

In conflict with such models, other data suggest the true percentage of division-competent stem/progenitor cells in the mammary gland may be dramatically underestimated using common assays. For example, cell division in mature ducts and in the terminal end bud, a structure enriched in stem/progenitor cells, is dependent on epithelial-epithelial and epithelial-stromal interactions (Wiseman and Werb, 2002). In addition, stem cells may require the presence of a three-dimensional "stem cell niche" for maintenance and self-renewal (Chepko and Dickson, 2003). Other studies show that growth of normal epithelium is inhibited by the presence of nearby or pre-existing epithelial structures (Faulkin and Deome, 1960). Thus, assays using dissociated cells or the intact gland may not allow the developmental potential of otherwise division-competent stem/progenitor cells to be expressed. Perhaps most damaging to these models are elegant genetic and transplantation studies showing that functionally differentiated epithelial cells retain division competence, can give rise to both lumenal and myoepithelial cells upon transplantation, and can participate in the development of oncogene-driven mammary cancer (Boulanger et al., 2005; Wagner and Smith, 2005).

Short term transplantation assays using small fragments of intact mammary duct transplanted into epithelium-free fat pads of host mice offer an excellent opportunity to test the prevailing stem/progenitor cell model, and to explore the developmental plasticity of mammary epithelium (Chew and Hoshino, 1970). With small fragments (~1000 cells), three-dimensional structure and cell-cell interactions are largely maintained, while the inhibitory effects of neighboring epithelium are minimized. Thus, stem/progenitor cells should be in an environment more favorable to cell division. In addition, onset of regeneration can be timed precisely.

If division-competent stem/progenitor cells represent a small percentage of all epithelial cells, the initial rate of cell division in transplanted fragments should be low, similar to that of dissociated cells, and limited to relatively undifferentiated epithelial cell types defined previously by EM. However, if stem/progenitor cells can include more differentiated, yet division-competent cells, the initial rate of cell division in fragments should be higher than that observed in transplants of dissociated cells, and include a broader range of epithelial cell types. Preliminary data showing ~15% of epithelial cells proliferate by 24 hours support the latter model.

Results

Objective 1) ***To determine the full range of division-competent stem/progenitor mammary epithelial cell types participating in early gland regeneration.***

Fragment transplantation: We have completed a series of ductal fragment transplantation experiments to determine the timing of stem/progenitor cell activation during early regeneration

through 24 hours post-transplantation and have initiated transplants for later time points. We have characterized these transplants with a series of markers to begin to define their behavior.

Our initial experimental protocol called for Brdu injection and tissue harvest at 6 hour intervals. We have modified this protocol for the first 24 hours such that BrdU injection and tissue harvest have been performed at 4 hour intervals after transplantation. This change was instituted because we were concerned that we might miss critical early and/or transient events in the regenerative process. Our concerns appear to be well-founded.

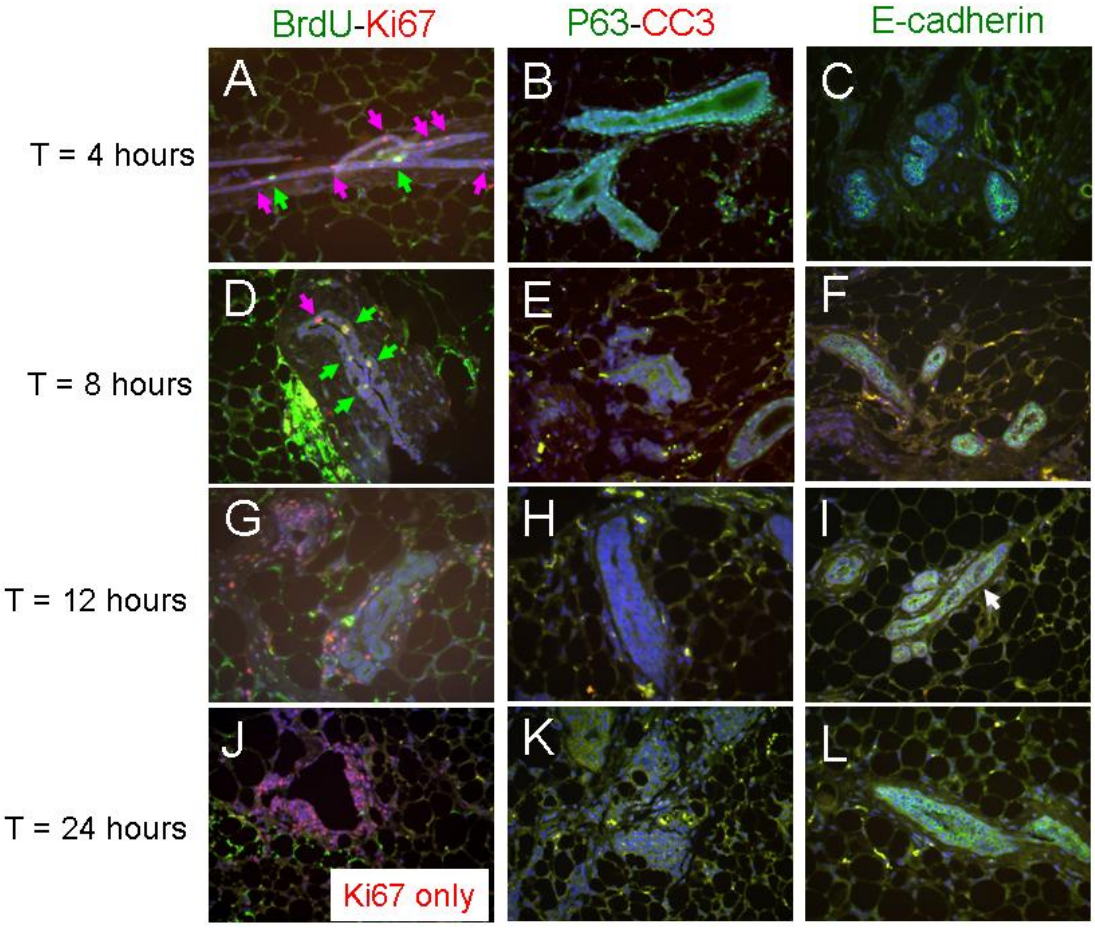

Figure 1. Changes in proliferation and marker expression during early mammary gland regeneration. Timepoint at harvest is denoted to the left of the row to which it applies. Marker assayed is denoted above the column to which it applies. Green arrows denote cells stained positively for BrdU incorporation with co-expression of Ki67. Magenta arrows denote cells expressing Ki67 exclusively. White arrow denotes an area of cells in which E-cadherin expression is reduced or lost.

Early regeneration appears to occur in a defined series of events. At 4 hours, there is a small burst of DNA synthesis in which ~2% of all epithelial cells in the transplant initiate DNA synthesis as determined by incorporation of BrdU and co-expression of Ki67 (Figure 1A). In addition, other cells enter the cell cycle based on expression of Ki67 alone (Figure 1A). At 8 hours, most cells expressing Ki67 also stain positive for incorporation of BrdU (Figure 1D). After this point, there is an approximately 16 hour period of relative growth quiescence (Figure 1G), followed by a second burst of proliferation at ~24 hours (Figure 1J). At this time ~15% of epithelial cells stain positively for expression of the Ki67 proliferation marker.

We also observed transient changes in gene expression in the myoepithelial cell layer. While all myoepithelial cells appear to express p63 at 4 hours (Figure 1B), at 8-20 hours, we observed reduction or loss of p63 expression in the myoepithelial cells (Figure 1E and 1H), which begins to be re-expressed at the 24 hour timepoint (Figure 1K). This loss of p63 expression was not due to

caspase-3 mediated apoptosis since we did not observe apoptotic cells in any of the transplanted fragments examined.

In the luminal cell layer, while epithelial cells at 4, 8 and 23 hours expressed E-cadherin in a relatively uniform pattern in all luminal epithelial cells (Figure 1C, 1F, and 1L), we observed transient reduction in the percentage of cells expressing E-cadherin, particularly at 12 hours (Figure 1I), with evidence to suggest reorganization of the epithelial cells within some of the transplanted fragments at the 12-24 hour timepoints.

Our interpretation of these data is that cells undergoing early DNA synthesis likely represent division-competent cells arrested at the G1/S restriction point of the cell cycle that, upon transplantation, were released from this cell cycle block and allowed to enter S-phase. Cells expressing Ki67 alone may have exited G0, but have not yet initiated DNA synthesis. By 8 hours, most of the Ki67+ cells have entered S-phase. These cells are most likely to be the same ER- progenitor cell types that one observes dividing in the mature gland normally, but are unlikely to represent true regenerative stem cells. Upon cellular reorganization, cells undergoing late DNA synthesis most likely represent regenerative stem cells and division-competent progenitor cells initiating the regeneration process. We are currently evaluating potential markers that might distinguish early and late S-phase cells from one another and from non-dividing cell types.

Loss of p63 expression from the myoepithelial cells and reduction/loss of E-cadherin expression from luminal epithelial cells was unexpected and indicates a degree of plasticity of both cell types. It is possible that both events influence the regeneration process. Thus, it would be of interest to see how sustained expression of either protein affected early regeneration. Our prediction is that sustained expression would delay onset of regeneration.

There are a number of technical limitations to these studies that we are attempting to overcome. The primary limitation is the small number of cells present in the transplanted fragments. The small size of the transplants makes them exceptionally difficult to find for conducting immunofluorescence analysis. We are therefore using epithelium genetically tagged to express enhanced cyan fluorescent protein (ECFP), which affords the opportunity to localize the transplanted duct fragment roughly within a given gland. We have begun to use 0.5mm skin biopsy punches to isolate the region containing the transplanted fragment coupled with use of tissue microarrays of multiple fragments from a given timepoint to enhance our ability to characterize regeneration events.

In addition to the difficulty in localizing transplanted epithelium, the small fragment size means that samples are exhausted quickly during microtomy, thus requiring numerous transplants for each timepoint. Finally, while putative stem cell markers have been published recently, all putative stem/progenitor cell markers used currently rely on subtle differences in fluorescence intensity in flow cytometric analysis using thousands of cells. Flow cytometric analysis is not possible for small fragments such as those being analyzed in this study (n<1000 cells/fragment). Thus, new markers are required that can be used in immunofluorescence analysis. We are attempting to identify such markers using a candidate gene approach.

***Mammosphere-formation and Limiting-dilution transplantation*:** In addition, to the fragment transplantation experiments, we have spent considerable effort to optimize mammosphere-formation and limiting dilution transplantation protocols for analysis of stem cell function in both wild type and mutant mice. We have used these techniques to compare stem cell function in FVB mice and our new *MMTV-SmoM2* mice expressing a constitutively activated form of Smoothened, the main effector of activated hedgehog signaling.

To determine whether *MMTV-SmoM2* transgenic mice showed a change in the frequency of mammosphere-forming cells relative to wild type controls, we conducted primary mammosphere-formation assays (Dontu et al., 2003; Dontu and Wicha, 2005). Using normal human mammary epithelial cells, mammospheres can be produced both by cells with multilineage differentiation capacity (a surrogate test for stem cells, presumably having regenerative potential), as well as by division-competent cells with either luminal or myoepithelial differentiation capacity (presumably lacking regenerative potential). In four of five independent paired primary cell preparations, cells

derived from *MMTV-SmoM2* mice showed a ~2-fold increase in the percentage of cells capable of forming primary mammospheres (mean raw value = 0.76%) relative to cells isolated from wild type littermate control mice (mean raw value = 0.38%) (P=0.02, paired-t test) (Figure 2A and 2B). There were no differences in mammosphere size or shape noted between the two genotypes (Figure 2C).

To verify that primary mammospheres contained regenerative mammary epithelial stem cells, we transplanted single mammospheres derived from wild type and *MMTV-SmoM2* mice into contralateral cleared fat pads of three-week old host mice. Mammospheres derived from both genotypes showed regenerative potential, with 2/13 (15%) of wild type mammospheres (Figure 2D, left panel), and 5/15 (33%) of *MMTV-SmoM2* mammospheres (Figure 2D, right panel) capable of regenerating ductal trees. These regeneration frequencies were not statistically different from one another (P=0.40, Fisher's exact test). Duct morphology in *MMTV-SmoM2* outgrowths was consistently altered relative to wild type in a manner consistent with the phenotype observed in intact mice.

A

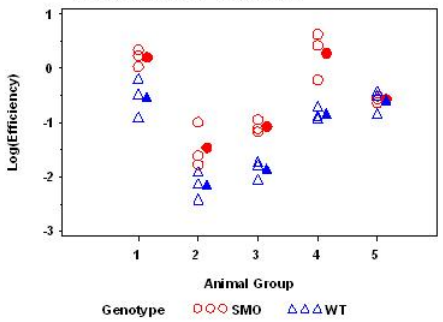

B

Table 2. Statistical Evaluation of Primary Mammosphere-forming Efficiency As a Function of Genotype.

	T-Tests		
Difference	*DF*	*t Value*	*Pr > |t|*
SMO - WT	**4**	**3.67**	**0.0214**

C

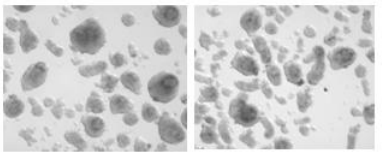

+/+ *MMTV-SmoM2*

D

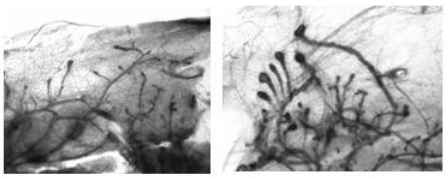

+/+ *MMTV-SmoM2*

E

Table 3. Limiting dilution transplantation analysis as a function of genotype.

	Genotype of epithelial cell donor			
	Wild type		*MMTV-SmoM2*	
Number of cells injected	Take rate	% fat pad filled	Take rate	% fat pad filled
1000	100% (4/4)	87.5 ±15.0	75% (3/4)	90 ±10.0
500	100% (10/10)	95 ±8.5	90% (9/10)	90 ±14.1
200	63% (5/8)	52 ±35.6	63% (5/8)	78 ±38.3
100	65% (11/17)	80 ±16.7	47% (8/17)	53.3 ±29.7
50	47% (7/15)	80 ±27.7	13% (2/15)	50 ±28.3
25	27% (4/15)	20 ±14.1	7% (1/15)	5 ±0.0
Regenerative stem cell frequency (upper and lower limits)	1/106 cells (1/72-1/156)		1/255 cells (1/166-1/390)	

F

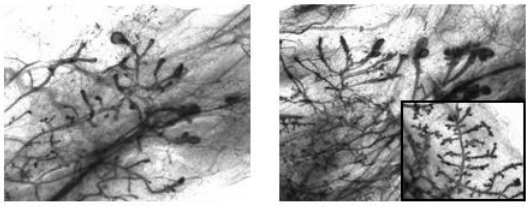

+/+ *MMTV-SmoM2*

Figure 2. Effect of *MMTV-SmoM2* on mammosphere formation and regeneration of the mammary gland. A. Pairwise comparison of log-transformed mammosphere-formation efficiency values for five paired sets of primary epithelial cell preparations. *MMTV-SmoM2* cells showed a two-fold increase in mammosphere-forming efficiency relative to wild type cells in four of the five sample pairs. B. Statistical evaluation of mammosphere-forming efficiency including all five paired samples shown in A. C. Photomicrographs of representative mammospheres from *MMTV-SmoM2* and wild type mice. D. Photomicrographs of representative outgrowths of transplanted mammospheres derived from wild type and *MMTV-SmoM2* mice. E. Limiting dilution transplantation analysis as a function of genotype. F. Photomicrographs of representative outgrowths from limiting dilution transplantations (100 cells).

Because mammosphere-formation assays are an indirect measure of the frequency of stem and progenitor cells present in the intact mammary gland, and because single mammosphere transplants showed no difference in regeneration frequency, it was possible that the two-fold increase in mammosphere-forming efficiency in cells derived from *MMTV-SmoM2* mice might not

be due to an increased proportion of regenerative stem cells in vivo, but rather due to an increase in the survival (or activity) of mammosphere-initiating cells under anchorage-independent growth conditions. To address this possibility, we conducted limiting dilution transplantation analysis designed to detect differences in the proportion of cells with regenerative capacity directly (Figure 2E).

We were fortunate enough to find a protocol quickly that allows for a transplant efficiently approximately one order of magnitude better than any published result (e.g. 1 regenerative stem cell per 1,400-2000 cells) – and is therefore in much better agreement with our fragment transplantation analyses. In this method, single cell suspensions of primary mammary epithelial cells are diluted into phosphate-buffered saline instead of tissue culture medium. After dilution, cells are mixed 1:1 (v/v) with Matrigel and injected in a 10ul volume. Injected glands are harvested 8 weeks post-transplantation and evaluated for growth of mammary glands.

For both genotypes, as few as 25 cells were capable of regenerating ductal trees. However, the rate of successful transplantation, or "take rate", was lower in cells derived from *MMTV-SmoM2* mice below 200 cells/gland injected. Using a single-hit Poisson distribution model (Bonnefoix et al., 1996), we estimate the frequency of regenerative stem cells in wild type epithelium is 1 stem cell per 106 cells (Figure 2E). The frequency of regenerative stem cells in *MMTV-SmoM2* epithelium was decreased ~2.5 fold, to 1 stem cell per 255 cells. Again, duct morphology in *MMTV-SmoM2* outgrowths was consistently altered relative to wild type (Figure 2F).

A manuscript summarizing these results has been submitted for publication to Development as part of our analysis of a new transgenic mouse model for hedgehog signaling activation (MMTV-SmoM2) (see below) and is currently under review.

Objective 2) To develop the short-term transplantation assay as a means by which critical regulators of stem and progenitor cell behavior can be discovered and evaluated.

Based on our optimized results from Objective 1, we are now in the position to be able to test our hypothesis rigorously using tissue fragments and cells derived from the MMTV-Wnt1 transgenic mouse model, as well as our new MMTV-SmoM2 transgenic mouse model (constitutively activated hedgehog signaling) (Moraes et al. submitted to Development). The MMTV-Wnt1 model was shown to possess an increased number of regenerative stem cells by limiting-dilution transplantation (though using a different method than that developed by us). Our MMTV-SmoM2 model shows an increase in the proportion of mammosphere-initiating cells (stem and progenitor cells), but a decrease in the proportion of regenerative stem cells in our optimized limiting-dlilution transplantation assay (Moraes et al. submitted to Development). Thus, we will have two bona-fide mouse models with which to test our initial hypothesis – one that increases regenerative capacity, and one that decreases regenerative capacity.

Key research accomplishments

1. Temporal characterization of early mammary gland regeneration through 24 hours with respect to BrdU incorporation and Ki67 expression.
2. Discovery of phenotypic plasticity of both luminal and myoepithelial cells during early regeneration with respect to p63 expression (myoepithelium) and E-cadherin expression (luminal epithelium), which offers some mechanistic insight into the early regeneration process since p63 is essential for mammary gland growth.
3. Optimization of limiting dilution transplantation and refinement of the estimate for the frequency of regenerative stem cells in the wild type gland relative to a new transgenic mouse line, MMTV-SmoM2, which shows a two-fold depletion in the frequency of regenerative stem cells.
4. Formal demonstration that about 1/3 of mammospheres contain, and therefore arise from, regenerative stem cells.

5. Formal demonstration that the mammosphere assay underestimates the true frequency of regenerative stem cells in the mouse mammary gland.

Reportable outcomes

Manuscripts

1. Ricardo C. Moraes, Xiaomei Zhang, Nikesha Harrington, Jennifer Y. Fung, Meng-Fen Wu, Susan G. Hilsenbeck, D. Craig Allred, and Michael T. Lewis. Constitutive Activation of *Smoothened (Smo)* in Mammary Glands of Transgenic Mice Leads to Increased Proliferation, Altered Differentiation, and Ductal Dysplasia. Development (In review)

Invited Presentations

1. Michael T. Lewis. Hedgehog signaling in mammary gland development. Think Tank 16. January 2005.
2. Michael T. Lewis. Hedgehog signaling in mammary stem cells. Cold Spring Harbor Research Workshop. December 2005.

Conclusions

Short-term transplantation appears to give a better estimate of the frequency of division-competent cells present in the gland than traditional assays. If suitable markers can be identified that can distinguish regenerative stem cells from downstream progenitor cells, the short-term transplantation assay may be a useful and rapid method for quantifying changes in the relative proportion of these cells due to mutation or treatment with bioactive compounds.

Analysis of the first events of mammary gland regeneration should allow identification of regulatory signaling networks and other regulatory mechanisms that govern stem and progenitor cell self-renewal.

References

Bonnefoix, T., Bonnefoix, P., Verdiel, P. and Sotto, J. J. (1996). Fitting limiting dilution experiments with generalized linear models results in a test of the single-hit Poisson assumption. *J Immunol Methods* **194**, 113-9.

Boulanger, C. A., Wagner, K. U. and Smith, G. H. (2005). Parity-induced mouse mammary epithelial cells are pluripotent, self-renewing and sensitive to TGF-beta1 expression. *Oncogene* **24**, 552-560.

Chepko, G. and Dickson, R. B. (2003). Ultrastructure of the putative stem cell niche in rat mammary epithelium. *Tissue Cell* **35**, 83-93.

Chew, E. C. and Hoshino, K. (1970). Early histogenesis of transplanted mouse mammary glands. II. Within 96 hours following isografting. *Z Anat Entwicklungsgesch* **132**, 318-24.

Clarke, R. B., Anderson, E., Howell, A. and Potten, C. S. (2003). Regulation of human breast epithelial stem cells. *Cell Prolif* **36 Suppl 1**, 45-58.

Dontu, G., Abdallah, W. M., Foley, J. M., Jackson, K. W., Clarke, M. F., Kawamura, M. J. and Wicha, M. S. (2003). In vitro propagation and transcriptional profiling of human mammary stem/progenitor cells. *Genes Dev* **17**, 1253-70.

Dontu, G. and Wicha, M. S. (2005). Survival of mammary stem cells in suspension culture: implications for stem cell biology and neoplasia. *J Mammary Gland Biol Neoplasia* **10**, 75-86.

Faulkin, L. J., Jr. and Deome, K. B. (1960). Regulation of growth and spacing of gland elements in the mammary fat pad of the C3H mouse. *J Natl Cancer Inst* **24**, 953-69.

Shackleton, M., Vaillant, F., Simpson, K. J., Stingl, J., Smyth, G. K., Asselin-Labat, M. L., Wu, L., Lindeman, G. J. and Visvader, J. E. (2006). Generation of a functional mammary gland from a single stem cell. *Nature* **439**, 84-8.

Smith, G. H. and Boulanger, C. A. (2003). Mammary epithelial stem cells: transplantation and self-renewal analysis. *Cell Prolif* **36 Suppl 1**, 3-15.

Stingl, J., Eirew, P., Ricketson, I., Shackleton, M., Vaillant, F., Choi, D., Li, H. I. and Eaves, C. J. (2006). Purification and unique properties of mammary epithelial stem cells. *Nature*.

Wagner, K. U. and Smith, G. H. (2005). Pregnancy and stem cell behavior. *J Mammary Gland Biol Neoplasia* **10**, 25-36.

Wiseman, B. S. and Werb, Z. (2002). Stromal effects on mammary gland development and breast cancer. *Science* **296**, 1046-9.

Constitutive Activation of *Smoothened (Smo)* in Mammary Glands of Transgenic Mice Leads to Increased Proliferation, Altered Differentiation, and Ductal Dysplasia.

Ricardo C. Moraes, Xiaomei Zhang, Nikesha Harrington, Jennifer Y. Fung, Meng-Fen Wu, Susan G. Hilsenbeck, D. Craig Allred, and Michael T. Lewis*

Baylor Breast Center and

Department of Molecular and Cellular Biology

Room N1210; MS:BCM600

Baylor College of Medicine

One Baylor Plaza

Houston, TX 77030

TEL: (713)798-3296

FAX: (713)798-1673

E-mail: mtlewis@breastcenter.tmc.edu

- To whom correspondence should be addressed.

Word count: 6995

Key words: Smoothened, mammary gland, hedgehog, stem cell, progenitor cell, human breast cancer.

ABSTRACT

The hedgehog signaling network regulates pattern formation, proliferation, cell fate, and stem/progenitor cell self-renewal in many organs. Altered hedgehog signaling is implicated in 20-25% of all cancers, including breast. We demonstrated previously that heterozygous disruption of the gene encoding the *Patched-1* (PTCH1) hedgehog receptor, a negative regulator of *Smoothened* (SMO) in the absence of ligand, led to mammary ductal dysplasia in virgin mice. We now show that expression of activated human SMO (SmoM2) under the Mouse Mammary Tumor Virus (MMTV) promoter in transgenic mice leads to increased proliferation, altered differentiation, and ductal dysplasias distinct from those caused by *Ptch1* heterozygosity. SMO activation also increased the mammosphere-forming efficiency of primary mammary epithelial cells. However, limiting-dilution transplantation showed a decrease in the frequency of regenerative stem cells in *MMTV-SmoM2* epithelium relative to wild type, suggesting enhanced mammosphere-forming efficiency was due to increased survival or activity of division-competent cell types under anchorage-independent growth conditions, rather than an increase in the proportion of regenerative stem cells per se. In human clinical samples, altered hedgehog signaling occurs early in breast cancer development, with PTCH1 expression reduced in ~50% of ductal carcinoma in situ (DCIS) and invasive breast cancers (IBC). Conversely, SMO is ectopically expressed in 70% of DCIS and 30% of IBC. Surprisingly, in both human tumors and *MMTV-SmoM2* mice, SMO rarely colocalized with Ki67. Taken together, our data suggest that altered hedgehog signaling may contribute to breast cancer development by stimulating proliferation, and by increasing the pool of division-competent cells capable of anchorage-independent growth.

INTRODUCTION

The hedgehog signaling network regulates pattern formation, proliferation, cell fate, and stem/progenitor cell maintenance and self-renewal in many organs (Cohen, 2003; Hooper and Scott, 2005; Lewis and Veltmaat, 2004; Nusse, 2003). Genetic analyses in mice indicate a role in mammary ductal morphogenesis, and recent data suggest a role in human mammary epithelial stem cell self-renewal (Liu et al., 2006). In addition to hedgehog functions in normal development, altered hedgehog signaling is now implicated in approximately 20-25% of all cancers (Briscoe and Therond, 2005), and there is increasing evidence to suggest a role in breast cancer (Chang-Claude et al., 2003; Kubo et al., 2004; Lewis et al., 2001; Lewis et al., 1999; Liu et al., 2006; Mukherjee et al., 2006; Naylor et al., 2005). However, the specific roles hedgehog network genes play in normal mammary gland development remain unclear, and no experiments have been performed to test directly whether inappropriately activated hedgehog signaling has functional consequences for gland development, or causes breast cancer.

Development of the mouse mammary gland begins in the embryo with formation of a rudimentary ductal tree, but most development occurs after puberty (Daniel, 1987; Sakakura, 1987). At puberty, ovarian steroids stimulate rapid and invasive ductal elongation and branching morphogenesis. At the growing tips of elongating ducts are bulb-like structures called terminal end buds (TEB). Histologically, TEBs consist of two highly proliferative cell compartments, an outer “cap cell” compartment, and an inner “body cell” compartment consisting of 4-6 layers of relatively undifferentiated luminal epithelial cells. As the TEB invades the mammary fat pad, cap cells serve as a progenitor cell population and differentiate into myoepithelial cells that line the basement membrane (Williams and Daniel, 1983), while body cells are thought to give rise to all luminal epithelial cell subtypes, including new multipotent mammary stem cells, of the mature duct. As ducts elongate, they are surrounded by a periductal stroma consisting of fibroblasts, macrophages, eosinophils, and vascular cells, within the confines of the mammary fat pad.

Hedgehog signaling involves two types of cells, a signaling cell expressing a member of the hedgehog family of secreted ligands (*Sonic Hedgehog* (SHH), *Indian Hedgeho*g (IHH), or *Desert Hedgehog* (DHH)), and a responding cell expressing one or more *Patched* family hedgehog receptors (*Patched-1* (PTCH1) and *Patched-2* (PTCH2)). In the absence of ligand, PTCH1 can function to inhibit downstream signaling via the *Smoothened* (SMO) transmembrane effector protein. Under these conditions, expression of hedgehog target genes is inhibited by repressor forms of one or more members of the *Gli* family of transcription factors (GLI2 or GLI3). In the presence of ligand, PTCH1 releases inhibition of SMO, which leads to induction of target genes by transcriptional activator forms of *Gli* transcription factors (GLI1, GLI2, or GLI3). In addition to its signal transduction activities, PTCH1 can also function to sequester hedgehog ligand, thereby restricting the range over which free ligand can signal (reviewed in (Hooper and Scott, 2005)). Finally, there is evidence to suggest PTCH1 can function as a "dependence receptor" to induce apoptosis in cell types dependent on ligand-bound PTCH1 for survival (Chao, 2003; Guerrero and Ruiz i Altaba, 2003; Thibert et al., 2003).

Our laboratory previously demonstrated critical functions for *Ptch1* and *Gli2* in mammary ductal development (Lewis et al., 2001; Lewis et al., 1999; Lewis and Veltmaat, 2004). Heterozygous mutation of *Ptch1 (ΔPtch1/+)* led to ductal dysplasia in virgin mice characterized by multiple epithelial cell layers within the ducts (Lewis et al., 1999). Similarly, transplantation rescue of whole mammary glands from homozygous *Gli2*-null mouse embryos yielded ductal dysplasias (Lewis et al., 2001). However, for both *Ptch1* and *Gli2*, transplantation of mutant epithelium into a wild type stroma failed to recapitulate the phenotype observed in intact glands, suggesting that these two genes function primarily in the stroma to regulate epithelial cell behavior. Thus, despite developmentally regulated hedgehog network gene expression in the epithelial compartment (Lewis et al., 2001) a role for activated hedgehog signaling in the epithelium has not been demonstrated during ductal development (Gallego et al., 2002; Michno et al., 2003), and the consequences of inappropriate hedgehog signaling in the epithelium are not known.

Our published working model for hedgehog signaling in mammary ductal development (Lewis and Veltmaat, 2004) proposes that hedgehog signaling may function transiently in the body cell layer of the TEB, but that signaling must be prevented in differentiated ducts. Consistent with this hypothesis, Liu and colleagues (Liu et al., 2006) showed that treatment of human breast epithelium with recombinant hedgehog ligand increased both primary and secondary mammosphere formation (in vitro assays of anchorage-independent growth, and of self-renewal of stem and progenitor cell types (Dontu et al., 2003; Dontu and Wicha, 2005)), while treatment with the hedgehog signaling antagonist cyclopamine decreased mammosphere formation. In this paper, we examine the effect of sustained SMO-mediated hedgehog signaling during ductal elongation in virgin transgenic mice, and correlate our results with altered PTCH1 and SMO expression in human breast cancer. Taken together, our results are consistent with a role in mammary epithelial progenitor cell regulation, and suggest that ectopic hedgehog signaling may contribute to human breast cancer by stimulating proliferation, and by increasing the pool of division-competent cells capable of anchorage-independent growth.

MATERIALS AND METHODS

Generation of *MMTV-SmoM2* transgenic mice and other mouse strains used: Transgenic mice expressing constitutively activated human SMO under the control of the MMTV promoter *(Tg(MMTV-SmoM2)*) were generated by the Baylor College of Medicine Mouse Embryo Manipulation Core (Dr. Franco DeMayo, Director) in the inbred FVB background. The *MMTV-SmoM2* construct was a kind gift from Dr. Frederick de Sauvage (Genentech, Inc., South San Francisco). Mice carrying a targeted disruption allele of the *Ptch1* gene (allele $Ptch1^{tm1Mps}$) were a generous gift from Dr. Matthew Scott (Stanford University), and were maintained by backcrossing to B6D2F1 mice. Genotype determination for the *Ptch1* disruption allele was performed as described previously (Lewis et al., 1999). All mice were maintained in accordance with the NIH Guide for the Care and Use of Experimental Animals with approval from our Institutional Animal Care and Use Committee.

Screening *MMTV-SmoM2* transgenic founder lines: Purified tail DNA from founders was used for PCR analysis for the presence of the *MMTV-SmoM2* transgene. Primers used were: forward (5'-GAGCTGCAGAAGCGCCTGGGCC-3') and reverse (5'-GGTATTGGTTCCTCTCTTTCCTG-3'). Cycling conditions were: 94˚C for 35 s, 62˚C for 40 s, and 72˚C for 50 s. Detection of a ~450 bp product indicated presence of the transgene. Of seven transgenic founder lines, five yielded progeny expressing the *MMTV-SmoM2* transgene by RT-PCR using RNA derived from surgical biopsies of the #4 mammary gland.

Five female mice per genotype per line were screened at 5 and 10 weeks of age for expression of *Smo* mRNA and protein, as well as for changes in ductal patterning, histology, proliferation, apoptosis, and expression of steroid hormone receptors. One line showing a representative ductal phenotype and proliferation rate (designated *Tg(MMTV-SmoM2)724Mtl*), and a line showing an identical ductal phenotype, but elevated proliferation rate (designated *Tg(MMTV-SmoM2)732Mtl)* were chosen for follow-up analysis (hereafter referred to as lines 724 and 732). Unless otherwise indicated, all data shown are for line 724.

Whole gland morphological analysis: Mammary glands #1-5 were harvested from the right side of at least 10 female mice at 5 and 10 weeks of age, as well as at >70 weeks of age (palpated weekly after 52 weeks of age to assay for tumor development), fixed in ice-cold 4% paraformaldehyde:PBS, and examined as whole mount preparations using a neutral red staining protocol. After fixation, fat was removed in three changes of acetone (1 hour each) and glands were stained in neutral red staining solution (0.01% neutral red in 100% EtOH acidified to pH 5.0 with glacial acetic acid) overnight with constant stirring. Glands were de-stained in 2 changes of 100% EtOH, cleared in two changes of xylenes (1 hour each), and stored in xylenes. Average terminal end bud (TEB) number per gland was quantified using the #3 mammary gland at 5 weeks of age. Branch point analysis and evaluation of retained TEB-like structures were conducted using the #3 mammary gland at 10 weeks of age by direct counting of all branchpoints.

Immunohistochemistry and immunofluorescence analysis: For histological analysis, the #2 and #3 mammary glands from the left side of the animal were fixed in 4% paraformaldehyde:PBS, embedded in paraffin, sectioned, and either hematoxylin/eosin stained or used for immunolocalization studies. Antibodies used for immunolocalization studies are listed in Table 1. All immunostaining was performed with antigen retrieval in 0.1M Tris-HCl, pH 9.0 with 10% Tween-20, or in TRS (DakoCytomation), by heating to 120°C, 10 min. in a pressure cooker. For immunohistochemistry, detection was by standard peroxidase staining using the ABC system (Vector Laboratories). For immunofluorescence, sections were counterstained with DAPI in mounting medium (Vectashield).

Primary mammary epithelial cell isolation: Primary mammary epithelial cells were isolated from freshly dissected mammary glands by enzymatic dissociation overnight in DMEM;Ham's F12 medium (5ml/mouse) containing collagenase (1mg/ml), hyaluronidase (100U/ml), penicillin/streptomycin (100U/ml), and gentamycin (50µg/ml) essentially as described (Smith, 1996). Resulting cell pellets were treated with 1ml 0.25% Trypsin-EDTA, 37°C, 5 minutes. Trypsin was inactivated with 10ml HBSS containing 5% serum. Cells were centrifuged and washed three times in

HBSS+5% serum. After the final wash, each preparation was filtered through a 40µm strainer to yield a single cell suspension. Single cell suspensions were used directly in mammosphere-formation assays and limiting-dilution transplantation assays.

Mammosphere-formation and transplantation assays: Primary mammary epithelial cells derived from five paired sets of wild type or *MMTV-SmoM2* mice (3-4 mice/genotype/set) were plated in triplicate wells of six-well ultra-low attachment plates (2ml/well) at a concentration of 30,000 cells/ml as described previously (Dontu et al., 2003; Youn et al., 2005). Cells were fed every 3-4 days for 10-14 days for mammospheres to form. Primary mammospheres were counted for each genotype, and the percentage of mammosphere-forming cells was calculated as a measure of mammosphere-forming efficiency.

To demonstrate that mammospheres contained stem cells capable of regenerating ductal trees, single mammospheres derived from wild type and *MMTV-SmoM2* mice were transplanted into contralateral cleared fat pads of three week old recipient FVB female mice (Deome et al., 1959). Transplanted mammospheres were allowed to grow for 6-8 weeks. Glands were then excised, fixed, and stained as whole mount preparations.

Limiting dilution cell transplantation assays: Primary mammary epithelial cells were isolated from 10 week old wild type and *MMTV-SmoM2* female mice, and counted on a hemocytometer. Cells were resuspended in a 1:1 solution of PBS:Matrigel (BD Biosciences 354234) at the desired concentration, and kept on ice until transplantation. Cells of each genotype were injected at limiting dilutions (1000, 500, 200, 100, 50, and 25 cells/gland in a total volume of 10µl) into contralateral cleared fat pads of the #4 mammary glands of 21-day-old female wild type mice using a 25G needle attached to a 50µl Hamilton glass syringe (Deome et al., 1959). Seven weeks after transplantation, #4 glands and a #3 host control gland were excised and stained as whole mounts. Glands showing ≥5% fat pad filling were scored as a positive “take”.

Human breast clinical samples: Low density tissue arrays comprised of archival formalin-fixed, paraffin-embedded samples of either ductal carcinoma in situ (DCIS), invasive breast cancer (IBC), or normal tissue derived from patients with breast cancer were used. All tissue was obtained, and used, with approval from our Institutional Review Board. DCIS samples had been scored previously for histological grade. Both DCIS and IBC samples had been scored previously for expression of estrogen receptor alpha (ERα), HER2/ERBB2, and p53 by the method of Allred (Allred et al., 1998; Harvey et al., 1999), in which a total score (0-8) is assigned as the sum of the proportion score (0-5), and an intensity score (0-3) for the expression of a given gene.

Quantitative RT-PCR: Total RNA was extracted using Trizol Reagent (Invitrogen). Total RNA (100ng/sample in triplicate) was reverse-transcribed (M-MLV Reverse Transcriptase, Invitrogen) following the manufacturer's protocol, and the resulting cDNA was analyzed using the Applied Biosystems 7500-Fast thermocycler for TaqMan® quantitative PCR (Q-PCR), using standard conditions. TaqMan® Assay On Demand primers and probes were purchased from Applied Biosystems. Product accumulation was evaluated using the comparative Ct method (ΔΔCt Method), with beta-actin as an endogenous control for normalization (Livak and Schmittgen, 2001).

Statistical analysis: Comparisons of gene expression levels across wild type and transgenic lines 724 and 732 were assessed by one-way ANOVA. Spearman correlation coefficients were calculated to assess associations between human SMO and the expression of mouse hedgehog network genes. Changes in hedgehog network gene expression in *ΔPtch1/+* animals relative to wild type were evaluated using a t-test.

For protein expression analyses, the average percentage of cells expressing a given protein in a given genetic background was compared to corresponding wild type controls using the Wilcoxon rank-sum test. For comparison of TEB number and branchpoint number between glands of wild type versus *MMTV-SmoM2* mice, mean numbers per gland were compared using a t-test. For mammosphere-

formation assays, mammosphere-formation efficiency values were log-transformed, and compared between paired groups of wild type and *MMTV-SmoM2* animals using a paired t-test.

Single mammosphere transplantation assays were performed to evaluate the frequency of mammospheres containing regenerative stem cells between wild type and *MMTV-SmoM2*. Regeneration frequencies were compared using Fisher's exact test.

Limiting dilution analysis was performed to estimate the frequency of regenerative stem cells in primary mammary epithelial cell preparations, along with 95% Wald confidence intervals (Smyth, 2006). The single-hit Poisson model (SHPM) was fitted to limiting dilution data using a complementary log-log generalized linear model (Bonnefoix et al., 1996).

In human clinical samples, correlations between expression of PTCH1 or SMO and clinically-relevant markers in DCIS, as well as that between PTCH1 and SMO in DCIS and IBC, were tested for statistical significance using Spearman's rank correlation. All of the variables in the correlation analysis were analyzed as continuous variables. Immunohistochemical total scores for expression of PTCH1 and SMO were compared between normal, DCIS, and IBC tissues using the Wilcoxon rank-sum test. Statistical analyses were performed with SAS (version 9.1), S-PLUS (version 7.0), or R (version 2.2.1). P-values of 0.05 or less were deemed statistically significant.

RESULTS

Ectopic SMO expression leads to mammary dysplasia in transgenic mice. Our working model of hedgehog network regulation of mammary ductal development proposes that the hedgehog signaling network may be active transiently in body cells of the TEB, but that signaling must be prevented in the epithelium of differentiated ducts (Lewis and Veltmaat, 2004). Thus, we hypothesized that constitutive activation in the epithelium might lead to altered ductal development, altered differentiation, and, perhaps, tumor formation. To test these hypotheses, we generated transgenic mice expressing a constitutively activated form of human SMO (Xie et al., 1998) selectively in mammary epithelium under the control of the MMTV promoter (Tg*(MMTV-SmoM2))*.

In whole mount analysis, glands of wild type mice at 5 weeks of age showed normal morphology of TEBs and subtending ducts (Figure 1A). In contrast, TEBs of *MMTV-SmoM2* mice frequently displayed excessive budding at the neck of the TEB (Figure 1B) and an increase in TEB number (Figure 1C) (P=0.05). In histological analyses, wild type glands showed normal TEB structure (Figure 1D). In contrast, ~30% of TEBs in *MMTV-SmoM2* glands showed disorganized cap and body cell layers (Figure 1E).

At 10 weeks of age, wild type ducts showed simple patterning and duct structure (Figure 1F). In contrast, *MMTV-SmoM2* transgenic mice showed one or more glands with enhanced side budding (Figure 1G) and increased branching by branch point analysis (Figure 1H) (P=0.04). Approximately 60% of transgenic mice showed retention of TEB-like structures (Figure 1G, inset, and Figure 1H).

At 10 weeks of age, ducts of wild type glands (Figure 1I) showed normal histoarchitecture with a single layer of lumenal epithelium and a single layer of myoepithelium. Ducts of *MMTV-SmoM2* glands showed histology consistent with increased side-budding, but appeared normal with respect to the lumenal and myoepithelial cell layers (Figure 1J), and did not show ducts having multiple layers of lumenal epithelium characteristic of *ΔPtch1/+* mice ((Lewis et al., 1999) and Figures 3E and 3F). Retained TEB-like structures showed histoarchitecture similar to TEBs, but the body cell layer was

generally only 2-4 cell layers thick (Figure 1J, inset). No tumors were detected in aged wild type virgin mice (n=15), and only a single tumor was detected in a cohort of aged transgenic virgin mice (n=77).

Our initial screen suggested that only a small percentage of epithelial cells in *MMTV-SmoM2* mice expressed detectable levels of SMO protein. Consistent with this observation, Q-PCR did not detect significant changes in hedgehog network gene expression, with the exception of decreased *Ptch1* (Figure 1, Supplemental). Because gene expression changes in a small number of cells can be masked using mRNA or protein derived from whole mammary glands, it was necessary to evaluate transgene expression and signaling activation by dual immunofluorescence analysis for SMO and PTCH1. Elevated expression of *Ptch1* – either mRNA or protein – can be observed in response to intermediate and high levels of hedgehog network activation (Hooper and Scott, 2005). Whereas SMO was undetectable in ducts of wild type glands at 10 weeks of age (Figure 2A), PTCH1 was detected, with near-uniform expression, in all epithelial cells (Figure 2B and 2C). In *MMTV-SmoM2* mice, ducts with altered morphology showed detectable SMO protein expression (Figure 2D). However, ducts expressing SMO were not necessarily altered morphologically. Staining was mosaic, with a median of only 5.7% of all epithelial cells showing detectable SMO expression (Figure 2F). PTCH1 expression in SMO expressing cells was not generally altered relative to adjacent SMO-negative cells. However, individual cells expressing relatively high levels of SMO showed increased PTCH1 expression relative to adjacent cells, consistent with intermediate-to-high levels of signaling activation in those cells (Figure 2E and 2F).

PTCH1 loss and SMO activation increase proliferation in the mammary gland in vivo. We next compared BrdU incorporation rates and expression patterns for cleaved caspase-3, ER, and PR, using glands of 10 week old *MMTV-SmoM2*, *ΔPtch1/+*, and wild type control mice (Figure 3 and Table 1 Supplemental). We detected no change in ER or PR expression between wild type and either *MMTV-SmoM2* or *ΔPtch1/+* mice, but detected a significant increase in BrdU incorporation in both

MMTV-SmoM2 (4.4%) and *ΔPtch1/+* mice (11.3%) relative to wild type age-matched littermate controls (~0.6%) (Figure 3A vs. 3C and 3E). Elevated BrdU incorporation rates in *MMTV-SmoM2* glands were corroborated by Ki67 staining, which was detected in 6.2% of wild type cells (Figure 3A inset), but in 31.3% of cells in *MMTV-SmoM2* glands (Figure 3C inset, and Table 1 Supplemental).

Because the *MMTV-SmoM2* mutant did not recapitulate the *ΔPtch1/+* phenotype, we expected to observe a compensatory increase in cell death to offset increased proliferation. Wild type glands showed low levels of cleaved caspase-3 staining (<1%) (Figure 3B). Contrary to expectations, *MMTV-SmoM2* mice did not show increased caspase-3-mediated apoptosis (Figure 3D). Glands from *ΔPtch1/+* mice also showed no change in cleaved caspase-3 expression as a percentage of total epithelial cells (Figure 3F). Thus, the reason proliferating cells accumulate in glands of *ΔPtch1/+* mice, but do not accumulate in glands of *MMTV-SmoM2* mice, remains unclear.

***MMTV-SmoM2* transgene expression and proliferation do not colocalize.** The observation that SMO expression was limited, yet morphological defects and expression of proliferation markers were wide-spread, led us to question to what degree transgene expression correlated with proliferation and hormone receptor status. We therefore conducted dual immunofluorescence staining for SMO, Ki67, and ER, and quantified co-expression in pairwise combinations. Overall, SMO was expressed in 5.7% of all epithelial cells, while Ki67 was expressed in 31.3% of epithelial cells. However, SMO and Ki67 did not colocalize (Figure 4A). We also found that SMO expression did not colocalize with ER (Figure 4B), with 33.0% of cells showing ER expression exclusively. Unlike wild type glands, ER and Ki67 colocalized at a low, but measurable, frequency (1.0%) in glands of transgenic mice (Figure 4C), (Table 1 Supplemental). Proliferation in ER-positive cells was confirmed by co-staining for ER and BrdU (Figure 4C, inset).

***MMTV-SmoM2* mice show altered epithelial cell differentiation.** Cytokeratin 6 (CK6), a marker of primitive progenitor cells (Grimm et al., 2006; Stingl et al., 2005), is expressed primarily in ER-positive cells in the body cell layer of the TEB, and only rarely in differentiated ducts of mature

glands (Grimm et al., 2006). As expected, in mature ducts of 10 week old wild type mice, expression of SMO was undetectable and CK6 was observed infrequently (7.5%), and at very low levels (Table 1 Supplemental). However, in 10 week old *MMTV-SmoM2* mice, CK6 expression was readily detectable in ~20% of epithelial cells (Figure 4D and 4E). Co-staining of CK6 and ER demonstrated that the majority of CK6+ cells (82.0%) were also ER+ (Figure 4D). There was no co-localization of SMO with CK6 (Figure 4E with inset). Thus, the *MMTV-SmoM2* transgene was expressed to detectable levels only in non-proliferative ER-CK6- cells.

***MMTV-SmoM2* increases the proportion of mammosphere-forming cells in mammary glands of transgenic mice in vivo.** To determine whether *MMTV-SmoM2* transgenic mice showed a change in the frequency of mammosphere-forming cells relative to wild type controls, we conducted primary mammosphere-formation assays (Dontu et al., 2003; Dontu and Wicha, 2005). Using normal human mammary epithelial cells, mammospheres can be produced both by cells with multilineage differentiation capacity (a surrogate test for stem cells, presumably having regenerative potential), as well as by division-competent cells with either luminal or myoepithelial differentiation capacity (presumably lacking regenerative potential). In four of five independent paired primary cell preparations, cells derived from *MMTV-SmoM2* mice showed a ~2-fold increase in the percentage of cells capable of forming primary mammospheres (mean raw value = 0.76%) relative to cells isolated from wild type littermate control mice (mean raw value = 0.38%) (P=0.02, paired-t test) (Figure 5A and 5B). There were no differences in mammosphere size or shape noted between the two genotypes (Figure 5C).

To verify that primary mammospheres contained regenerative mammary epithelial stem cells, we transplanted single mammospheres derived from wild type and *MMTV-SmoM2* mice into contralateral cleared fat pads of three-week old host mice. Mammospheres derived from both genotypes showed regenerative potential, with 2/13 (15%) of wild type mammospheres (Figure 5D, left panel), and 5/15 (33%) of *MMTV-SmoM2* mammospheres (Figure 5D, right panel) capable of

regenerating ductal trees. These regeneration frequencies were not statistically different from one another (P=0.40, Fisher's exact test). Duct morphology in *MMTV-SmoM2* outgrowths was consistently altered relative to wild type in a manner consistent with the phenotype observed in intact mice.

***MMTV-SmoM2* transgene expression decreases the frequency of regenerative stem cells in vivo**. Because mammosphere-formation assays are an indirect measure of the frequency of stem and progenitor cells present in the intact mammary gland, and because single mammosphere transplants showed no difference in regeneration frequency, it was possible that the two-fold increase in mammosphere-forming efficiency in cells derived from *MMTV-SmoM2* mice might not be due to an increased proportion of regenerative stem cells in vivo, but rather due to an increase in the survival (or activity) of mammosphere-initiating cells under anchorage-independent growth conditions. To address this possibility, we conducted limiting dilution transplantation analysis designed to detect differences in the proportion of cells with regenerative capacity directly (Figure 5E).

For both genotypes, as few as 25 cells were capable of regenerating ductal trees. However, the rate of successful transplantation, or "take rate", was lower in cells derived from *MMTV-SmoM2* mice below 200 cells/gland injected. Using a single-hit Poisson distribution model (Bonnefoix et al., 1996), we estimate the frequency of regenerative stem cells in wild type epithelium is 1 stem cell per 106 cells (Figure 5E). The frequency of regenerative stem cells in *MMTV-SmoM2* epithelium was decreased ~2.5 fold, to 1 stem cell per 255 cells. Again, duct morphology in *MMTV-SmoM2* outgrowths was consistently altered relative to wild type (Figure 5F).

Hedgehog signaling is altered at high frequency in human breast cancer. To evaluate a potential role for PTCH1 and SMO in human breast cancer, we conducted an immunohistochemical study for expression of PTCH1 and SMO in a panel of normal, DCIS, and IBC samples (Figure 6 and Table 4). PTCH1 was detectable throughout the epithelium (Figure 6A), and in isolated stromal cells of the normal breast. In contrast, PTCH1 expression was decreased or absent in ~50% of ductal carcinoma in situ (DCIS) (Figure 6B) and invasive breast cancers (IBC) (Figure 6C). Conversely,

SMO was undetectable in normal breast (Figure 6D), but ectopically expressed in ~70% of DCIS and ~30% of IBC (Figures 6E and 6F). For both proteins, total scores between DCIS and IBC were significantly different from each other (SMO: P=0.0003, PTCH1: P=0.0001, Wilcoxon rank sum test) (Table 4). By Spearman rank correlation analysis, expression of PTCH1 or SMO did not correlate with histological grade (DCIS only) or with expression of any clinically-relevant marker tested. PTCH1 expression was not significantly correlated with SMO expression in either DCIS or IBC.

SMO-positive cells are rarely proliferative in human breast cancer. To explore the relationship between PTCH1 or SMO expression and proliferation in human breast cancers, we conducted dual immunofluorescence analysis of PTCH1-Ki67, and of SMO-Ki67, in both DCIS (Figure 7A-C and G-H) and IBC (Figure 7D-F and I-J). Lesions in which PTCH1 expression was low-to-undetectable showed varying degrees of Ki67 staining (Figures 7A and 7D). In tumors expressing PTCH1 (Figure 7B, 7C, 7E, and 7F), there was extensive colocalization with the Ki67 proliferation marker. However, in tumors expressing SMO (Figure 7G-J), SMO expression rarely colocalized with the Ki67 proliferation marker (Figure 7K).

DISCUSSION

In this paper, we show that expression of constitutively activated human SMO (SmoM2) under the MMTV promoter in transgenic mice leads to ductal dysplasias distinct from those caused by Δ*Ptch1* heterozygosity, despite increased in proliferation in both models. SMO expression rarely colocalized with the Ki67 proliferation marker, and activation was not sufficient to cause tumors at high frequency. SMO activation led to altered differentiation, as well as enhanced primary mammosphere-forming efficiency. However, limiting-dilution transplantation analysis showed a decrease in the frequency of regenerative stem cells in *MMTV-SmoM2* epithelium relative to wild type. In human clinical samples, hedgehog network gene expression is altered frequently, and early, in breast cancer development. As in *MMTV-SmoM2* mice, SMO rarely colocalized with Ki67 in breast tumors. Taken together, these data are consistent with our model that hedgehog signaling must be prevented in mature ducts of virgin mice, and suggests that it is also inactive normally in mature ducts in humans. Thus, ectopic hedgehog signaling could contribute to early breast cancer development by stimulating proliferation, and by increasing the pool of division-competent cells capable of anchorage-independent growth.

In light of our transplantation results published previously (Lewis et al., 1999), failure of *MMTV-SmoM2* to recapitulate the *ΔPtch1* hyperplastic phenotype was not entirely unexpected. In these experiments, the *ΔPtch1/+* phenotype could be partially recapitulated, but only when the entire mammary gland was transplanted -- transplantation of epithelial fragments into cleared fat pads of wild type mice did not lead to ductal dysplasia. These results led to the interpretation that the *ΔPtch1/+* phenotype was due primarily to loss-of-function in mammary stroma. Since the *MMTV-SmoM2* transgene is expressed selectively in the mammary epithelium, stromal activation of hedgehog signaling was not tested here. Thus, the two models are not directly comparable. However, our results clearly demonstrate that *ΔPtch1* heterozygosity is not functionally equivalent to SMO activation solely in mammary epithelium.

In 10 week old *MMTV-SmoM2* mice, we demonstrate altered gland morphology in whole mount preparations, as well as widespread changes in marker expression (Ki67, BrdU, and CK6) throughout histological preparations of affected glands. However, only ~5.7% of all epithelial cells expressed detectable levels of SMO protein. There are at least three possible interpretations of these results.

First, the simplest interpretation is that SMO is, in fact, only expressed and active in a small percentage of cells in *MMTV-SmoM2* mice. This interpretation is consistent with the small number of strongly stained SMO+ cells showing evidence of increased PTCH1 expression relative to their immediate neighbors. This interpretation then leads to the intriguing hypothesis that SMO activity in these few cells promotes persistence of ER+CK6+ cells, and stimulates proliferation indirectly via an undefined paracrine signaling factor (or factors). This possibility is being evaluated in a series of in vitro cell mixing and in vivo transplantation experiments similar to those used to demonstrate paracrine signaling functions for the estrogen and progesterone receptors during mammary gland development (Brisken et al., 1998; Mallepell et al., 2006).

A second possibility is that SMO is expressed and active in >5.7% of cells, but that SMO protein expression is below the limit of detection. Consistent with this possibility, available antibodies must be used at relatively high concentrations, and fail to detect SMO in some tissues known have hedgehog signaling activity (e.g. E14 embryo, hair follicle, colon) (not shown). However, this interpretation requires the supposition that low-level activity is not sufficient to induce expression of PTCH1 in most cells (Hooper and Scott, 2005) (Figure 2 and Figure 1 Supplemental). Alternatively, it may be that the majority of mouse mammary epithelial cells are incompetent to respond to increased SMO activity. Indeed, with the exception of *Hip1*, whose expression by Q-PCR was increased 2-fold ($p=0.049$) above wild type, ***Δ****Ptch1* heterozygosity was also not sufficient to induce expression of other hedgehog network genes (Figure 1, Supplemental).

A third interpretation is that the primary effect of ectopic SMO expression occurs in, or near, the TEB and leads to a permanent alteration in cell fate. This would require that the permanent alteration lead to inactivation of the MMTV promoter such that it was no longer expressed. This possibility is being addressed using an conditional SMO overexpression model to activate signaling after ductal development is completed (Jeong et al., 2004).

With respect to normal mammary development, our data and those of Liu et al. (Liu et al., 2006) are consistent with our working model in which hedgehog signaling may be active in the growing TEB (extrapolated from *Ihh* and *Ptch1* in situ hybridization data showing low, but detectable expression of *Ihh* in the TEB, as well as increased *Ptch1* expression relative to the immediately subtending differentiated duct), but that signaling is normally absent from mature ducts of the wild type mice (Lewis and Veltmaat, 2004). Absence of activated hedgehog signaling in mature ducts is supported by reduced levels of *Ptch1* mRNA in differentiated ducts relative to the TEB, the lack of detectable SMO protein expression, and the failure to detect *Gli* gene function in mammary epithelium of postnatal animals (Hatsell and Cowin, 2006; Lewis et al., 2001; Lewis and Veltmaat, 2004). It remains possible that postnatal mammary duct formation is entirely hedgehog ligand-independent (discussed in (Lewis and Veltmaat, 2004)). However, the definitive experiments required to determine whether active hedgehog signaling functions in the epithelium during postnatal ductal development have never been performed. We are currently analyzing conditional null mutants of both *Ptch1* and *Smo*, which should allow us to test our model conclusively.

In *MMTV-SmoM2* mice, we observed a two-fold increase in the percentage of mammosphere-forming cells present in primary mammary epithelial cell cultures relative to wild type (Dontu et al., 2003; Youn et al., 2005). Unfortunately, a potential limitation of secondary mammosphere-formation assays for the evaluation of changes in self-renewal capacity in MMTV transgenic mice was revealed. In our hands, transgene expression was not detectable in primary mammospheres by immunofluorescence (not shown). Because of this, secondary mammosphere-formation assays to test

for changes in stem cell self-renewal as a consequence of transgene expression during primary mammosphere culture were not considered reliable. Thus, it is difficult to compare our mouse mammosphere-formation data directly with those of Liu et al (Liu et al., 2006) who demonstrated increased primary and secondary mammosphere formation in response to treatment with recombinant SHH ligand using human cells. We are currently repeating these experiments using mouse primary mammary epithelial cells to reconcile these two datasets.

Our limiting dilution transplantation assays showed decreased regenerative capacity in primary mammary epithelial cells isolated from *MMTV-SmoM2* mice relative to wild type, suggesting either a decrease in stem cell frequency, an impaired ability of stem cells to regenerate ductal trees, or both. Our interpretation of limiting dilution data in conjunction with the mammosphere-formation data is that, in the intact mammary gland in vivo, signaling activation via the *MMTV-SmoM2* transgene decreases regenerative stem cell frequency, but increases the survival or activity of division-competent cell types capable of anchorage independent growth. However, it remains possible that the MMTV promoter is not active in the most primitive stem cell (Welm et al., 2005), which might affect experimental outcome.

With respect to human breast disease, data are accumulating that suggest a role for altered hedgehog signaling in mammary tumorigenesis. An early study found *Ptc1* mutations in 2 of 7 human breast cancers (Xie et al., 1997). Additionally, a *Ptch1* polymorphism was linked to increased breast cancer risk associated with oral contraceptive use (Chang-Claude et al., 2003). More recently, array comparative genomic hybridization (CGH) analyses indicate that genomic loss at the *Ptch1* locus was the fourth most commonly detected change among the tumor suppressor genes identified in the study, occurring in 19% of human breast cancers, and 33% of breast cancer cell lines (Naylor et al., 2005). However, no mutations in other network components have been identified in breast cancer (Vorechovsky et al., 1999). A recent immunohistochemical staining study suggested that hedgehog signaling is activated in a majority of human invasive breast cancers based on ectopic expression of

PTCH1 and nuclear GLI1 (Kubo et al., 2004). Further, the hedgehog signaling inhibitor cyclopamine inhibited growth of some breast cell lines in vitro (Kubo et al., 2004; Mukherjee et al., 2006). However, the specificity of cyclopamine at the doses required for growth inhibition remains an open question (Mukherjee et al., 2006).

Our data showing loss of PTCH1 protein expression in ~50% of DCIS and IBC are most consistent with the array CGH results, but differ significantly from the immunohistochemical study by Kubo et al. (Kubo et al., 2004). In the Kubo study, PTCH1 was not detected in normal tissue, but was detected in 50 of 52 cancers examined. In contrast, we readily detect PTCH1 in normal breast, but expression was reduced or lost in about half of all tumors. The reason for the discrepancy is unclear since both studies used the same rabbit polyclonal antibody, but may be related to the different antigen retrieval strategies used. In our study, we used a second PTCH1 antibody (G-19) to confirm expression patterns in normal human and mouse mammary epithelium. In addition, we used isotype-matched rabbit IgG as a negative control (not shown). Since both PTCH1 antibodies yielded consistent expression patterns in both mouse and human tissue, and immunolocalization patterns in mouse were consistent with previous in situ hybridization data, we are reasonably confident in our results. Altered SMO expression in human breast cancer has not been demonstrated previously. Given that SMO was not detectable in normal human or mouse tissue, but was readily detectable in *MMTV-SmoM2* mice, we are confident of the specificity of the two antibodies used.

Our observation that SMO protein expression does not colocalize frequently with proliferation markers in either the *MMTV-SmoM2* mouse model or in human breast tumors was unexpected. These observations must be reconciled with data suggesting a direct role for hedgehog signaling in normal human stem cell self-renewal (Liu et al., 2006), and with reports that hedgehog signaling activation appears to increase proliferation directly in other cell types (e.g. (Detmer et al., 2005; Hutchin et al., 2005; MacLean and Kronenberg, 2005; Palma et al., 2005)). In any case, the similarity in staining patterns of SMO relative to proliferation markers in both the mouse and human models suggests that

our *MMTV-SmoM2* transgenic model reflects important aspects of human breast tumor biology, and that it will therefore be a useful model for studying the underlying mechanism of hedgehog network regulation of stem/progenitor cell behavior in mammary gland development and breast cancer.

LITERATURE CITED

Allred, D. C., Harvey, J. M., Berardo, M. and Clark, G. M. (1998). Prognostic and predictive factors in breast cancer by immunohistochemical analysis. *Mod Pathol* **11**, 155-68.

Bonnefoix, T., Bonnefoix, P., Verdiel, P. and Sotto, J. J. (1996). Fitting limiting dilution experiments with generalized linear models results in a test of the single-hit Poisson assumption. *J Immunol Methods* **194**, 113-9.

Briscoe, J. and Therond, P. (2005). Hedgehog signaling: from the Drosophila cuticle to anti-cancer drugs. *Dev Cell* **8**, 143-151.

Brisken, C., Park, S., Vass, T., Lydon, J. P., O'Malley, B. W. and Weinberg, R. A. (1998). A paracrine role for the epithelial progesterone receptor in mammary gland development. *Proc Natl Acad Sci U S A* **95**, 5076-81.

Chang-Claude, J., Dunning, A., Schnitzbauer, U., Galmbacher, P., Tee, L., Wjst, M., Chalmers, J., Zemzoum, I., Harbeck, N., Pharoah, P. D. et al. (2003). The patched polymorphism Pro1315Leu (C3944T) may modulate the association between use of oral contraceptives and breast cancer risk. *Int J Cancer* **103**, 779-83.

Chao, M. V. (2003). Dependence receptors: what is the mechanism? *Sci STKE* **2003**, PE38.

Cohen, M. M., Jr. (2003). The hedgehog signaling network. *Am J Med Genet* **123A**, 5-28.

Daniel, C. W. S., G.B. (1987). Developmental biology of the mammary gland. In *The Mammary Gland*, (ed. M. C. Neville and C. W. Daniel). New York: Plenum.

Deome, K. B., Faulkin, L. J., Jr., Bern, H. A. and Blair, P. B. (1959). Development of mammary tumors from hyperplastic alveolar nodules transplanted into gland-free mammary fat pads of female C3H mice. *Cancer Res* **19**, 515-20.

Detmer, K., Thompson, A. J., Garner, R. E., Walker, A. N., Gaffield, W. and Dannawi, H. (2005). Hedgehog signaling and cell cycle control in differentiating erythroid progenitors. *Blood Cells Mol Dis* **34**, 60-70.

Dontu, G., Abdallah, W. M., Foley, J. M., Jackson, K. W., Clarke, M. F., Kawamura, M. J. and Wicha, M. S. (2003). In vitro propagation and transcriptional profiling of human mammary stem/progenitor cells. *Genes Dev* **17**, 1253-70.

Dontu, G. and Wicha, M. S. (2005). Survival of mammary stem cells in suspension culture: implications for stem cell biology and neoplasia. *J Mammary Gland Biol Neoplasia* **10**, 75-86.

Gallego, M. I., Beachy, P. A., Hennighausen, L. and Robinson, G. W. (2002). Differential requirements for shh in mammary tissue and hair follicle morphogenesis. *Dev Biol* **249**, 131-9.

Grimm, S. L., Bu, W., Longley, M. A., Roop, D. R., Li, Y. and Rosen, J. M. (2006). Keratin 6 is not essential for mammary gland development. *Breast Cancer Res* **8**, R29.

Guerrero, I. and Ruiz i Altaba, A. (2003). Development. Longing for ligand: hedgehog, patched, and cell death. *Science* **301**, 774-6.

Harvey, J. M., Clark, G. M., Osborne, C. K. and Allred, D. C. (1999). Estrogen receptor status by immunohistochemistry is superior to the ligand-binding assay for predicting response to adjuvant endocrine therapy in breast cancer. *J Clin Oncol* **17**, 1474-81.

Hatsell, S. J. and Cowin, P. (2006). Gli3-mediated repression of Hedgehog targets is required for normal mammary development. *Development*.

Hooper, J. E. and Scott, M. P. (2005). Communicating with Hedgehogs. *Nat Rev Mol Cell Biol* **6**, 306-17.

Hutchin, M. E., Kariapper, M. S., Grachtchouk, M., Wang, A., Wei, L., Cummings, D., Liu, J., Michael, L. E., Glick, A. and Dlugosz, A. A. (2005). Sustained Hedgehog signaling is required for basal cell carcinoma proliferation and survival: conditional skin tumorigenesis recapitulates the hair growth cycle. *Genes Dev* **19**, 214-23.

Jeong, J., Mao, J., Tenzen, T., Kottmann, A. H. and McMahon, A. P. (2004). Hedgehog signaling in the neural crest cells regulates the patterning and growth of facial primordia. *Genes Dev* **18**, 937-51.

Kayed, H., Kleeff, J., Keleg, S., Buchler, M. W. and Friess, H. (2003). Distribution of Indian Hedgehog and its receptors patched and smoothened in human chronic pancreatitis. *J Endocrinol* **178**, 467-78.

Kayed, H., Kleeff, J., Keleg, S., Guo, J., Ketterer, K., Berberat, P. O., Giese, N., Esposito, I., Giese, T., Buchler, M. W. et al. (2004). Indian hedgehog signaling pathway: expression and regulation in pancreatic cancer. *Int J Cancer* **110**, 668-76.

Kubo, M., Nakamura, M., Tasaki, A., Yamanaka, N., Nakashima, H., Nomura, M., Kuroki, S. and Katano, M. (2004). Hedgehog signaling pathway is a new therapeutic target for patients with breast cancer. *Cancer Res* **64**, 6071-4.

Lewis, M. T., Ross, S., Strickland, P. A., Sugnet, C. W., Jimenez, E., Hui, C. and Daniel, C. W. (2001). The Gli2 transcription factor is required for normal mouse mammary gland development. *Dev Biol* **238**, 133-44.

Lewis, M. T., Ross, S., Strickland, P. A., Sugnet, C. W., Jimenez, E., Scott, M. P. and Daniel, C. W. (1999). Defects in mouse mammary gland development caused by conditional haploinsufficiency of Patched-1. *Development* **126**, 5181-93.

Lewis, M. T. and Veltmaat, J. M. (2004). Next stop, the twilight zone: hedgehog network regulation of mammary gland development. *J Mammary Gland Biol Neoplasia* **9**, 165-81.

Liu, S., Dontu, G., Mantle, I. D., Patel, S., Ahn, N. S., Jackson, K. W., Suri, P. and Wicha, M. S. (2006). Hedgehog signaling and Bmi-1 regulate self-renewal of normal and malignant human mammary stem cells. *Cancer Res* **66**, 6063-71.

Livak, K. J. and Schmittgen, T. D. (2001). Analysis of relative gene expression data using real-time quantitative PCR and the 2(-Delta Delta C(T)) Method. *Methods* **25**, 402-8.

Long, F., Zhang, X. M., Karp, S., Yang, Y. and McMahon, A. P. (2001). Genetic manipulation of hedgehog signaling in the endochondral skeleton reveals a direct role in the regulation of chondrocyte proliferation. *Development* **128**, 5099-5108.

MacLean, H. E. and Kronenberg, H. M. (2005). Localization of Indian hedgehog and PTH/PTHrP receptor expression in relation to chondrocyte proliferation during mouse bone development. *Dev Growth Differ* **47**, 59-63.

Mallepell, S., Krust, A., Chambon, P. and Brisken, C. (2006). Paracrine signaling through the epithelial estrogen receptor {alpha} is required for proliferation and morphogenesis in the mammary gland. *Proc Natl Acad Sci U S A* **103**, 2196-201.

Michno, K., Boras-Granic, K., Mill, P., Hui, C. C. and Hamel, P. A. (2003). Shh expression is required for embryonic hair follicle but not mammary gland development. *Dev Biol* **264**, 153-65.

Mukherjee, S., Frolova, N., Sadlonova, A., Novak, Z., Steg, A., Page, G. P., Welch, D. R., Lobo-Ruppert, S. M., Ruppert, J. M., Johnson, M. R. et al. (2006). Hedgehog signaling and response to cyclopamine differ in epithelial and stromal cells in benign breast and breast cancer. *Cancer Biol Ther* **5**, 674-83.

Naylor, T. L., Greshock, J., Wang, Y., Colligon, T., Yu, Q. C., Clemmer, V., Zaks, T. Z. and Weber, B. L. (2005). High resolution genomic analysis of sporadic breast cancer using array-based comparative genomic hybridization. *Breast Cancer Res* **7**, R1186-98.

Nusse, R. (2003). Wnts and Hedgehogs: lipid-modified proteins and similarities in signaling mechanisms at the cell surface. *Development* **130**, 5297-305.

Oniscu, A., James, R. M., Morris, R. G., Bader, S., Malcomson, R. D. and Harrison, D. J. (2004). Expression of Sonic hedgehog pathway genes is altered in colonic neoplasia. *J Pathol* **203**, 909-17.

Palma, V., Lim, D. A., Dahmane, N., Sanchez, P., Brionne, T. C., Herzberg, C. D., Gitton, Y., Carleton, A., Alvarez-Buylla, A. and Ruiz i Altaba, A. (2005). Sonic hedgehog controls stem cell behavior in the postnatal and adult brain. *Development* **132**, 335-44.

Sacedon, R., Varas, A., Hernandez-Lopez, C., Gutierrez-deFrias, C., Crompton, T., Zapata, A. G. and Vicente, A. (2003). Expression of hedgehog proteins in the human thymus. *J Histochem Cytochem* **51**, 1557-66.

Sakakura, T. (1987). Mammary embryogenesis. In *The Mammary Gland*, (ed. M. C. Neville and C. W. Daniel). New York: Plenum.

Smith, G. H. (1996). Experimental mammary epithelial morphogenesis in an in vivo model: evidence for distinct cellular progenitors of the ductal and lobular phenotype. *Breast Cancer Res Treat* **39**, 21-31.

Smyth, G. (2006). Statmod: Statistical Modeling. R package version 1.2.4., (ed.

Stingl, J., Raouf, A., Emerman, J. T. and Eaves, C. J. (2005). Epithelial progenitors in the normal human mammary gland. *J Mammary Gland Biol Neoplasia* **10**, 49-59.

Thibert, C., Teillet, M. A., Lapointe, F., Mazelin, L., Le Douarin, N. M. and Mehlen, P. (2003). Inhibition of neuroepithelial patched-induced apoptosis by sonic hedgehog. *Science* **301**, 843-6.

Vorechovsky, I., Benediktsson, K. P. and Toftgard, R. (1999). The patched/hedgehog/smoothened signalling pathway in human breast cancer: no evidence for H133Y SHH, PTCH and SMO mutations. *Eur J Cancer* **35**, 711-3.

Welm, A. L., Kim, S., Welm, B. E. and Bishop, J. M. (2005). MET and MYC cooperate in mammary tumorigenesis. *Proc Natl Acad Sci U S A* **102**, 4324-9.

Williams, J. M. and Daniel, C. W. (1983). Mammary ductal elongation: differentiation of myoepithelium and basal lamina during branching morphogenesis. *Dev Biol* **97**, 274-90.

Xie, J., Johnson, R. L., Zhang, X., Bare, J. W., Waldman, F. M., Cogen, P. H., Menon, A. G., Warren, R. S., Chen, L. C., Scott, M. P. et al. (1997). Mutations of the PATCHED gene in several types of sporadic extracutaneous tumors. *Cancer Res* **57**, 2369-72.

Xie, J., Murone, M., Luoh, S. M., Ryan, A., Gu, Q., Zhang, C., Bonifas, J. M., Lam, C. W., Hynes, M., Goddard, A. et al. (1998). Activating Smoothened mutations in sporadic basal-cell carcinoma. *Nature* **391**, 90-2.

Youn, B. S., Sen, A., Kallos, M. S., Behie, L. A., Girgis-Gabardo, A., Kurpios, N., Barcelon, M. and Hassell, J. A. (2005). Large-scale expansion of mammary epithelial stem cell aggregates in suspension bioreactors. *Biotechnol Prog* **21**, 984-93.

LEGENDS TO FIGURES

Figure 1. Whole mount and histological analysis of mammary glands from wild type and *MMTV-SmoM2* mice. A. Whole mount showing a normal TEB array from a wild type mouse at 5 weeks of age. Terminal structures are denoted by an asterisk (*); side-buds are denoted by arrows. B. Whole mount showing a TEB array from an *MMTV-SmoM2* transgenic mouse at 5 weeks of age. Symbols are as described in A. C. Quantification of TEB number in wild type versus *MMTV-SmoM2* mice at 5 weeks of age. D. Histological preparation of a TEB in a wild type gland showing organized cap and body cell layers, as well as normal periductal stroma condensing around the neck of the TEB (arrow). E. Histological preparation of TEB in an *MMTV-SmoM2* transgenic gland showing abnormal histology associated with the side-budding phenotype (arrow). TEB could also show disorganized cap and body cell layers (inset). F. Whole mount from a 10 week old wild type mouse showing normal duct patterning and blunt-ended ducts. G. Whole mount from a 10 week old *MMTV-SmoM2* mouse. Inset - Retained TEB-like structures. H. Branchpoint analysis and quantification of retained TEB-like structures at 10 weeks of age as a function of genotype. I. Histological preparation of a normal mature duct in a wild type gland. J. Histological preparation of a mature duct in an *MMTV-SmoM2* gland. Inset – Retained TEB-like structures. Scale bars: 50μm.

Figure 2. Dual immunofluorescence for SMO and PTCH1 in wild type (A, B, C) and *MMTV-SmoM2* transgenic (D, E, F) mammary glands. Individual panels are shown for each protein shown at the top of the column to which it applies, along with the merged three-color image including the DAPI counterstain. A. No detectable SMO expression. B. Near uniform PTCH1 expression. C. Merged image. D. Area of duct in a transgenic gland showing ectopic SMO expression. E. PTCH1 expression in the same duct showing cell-to-cell variation in PTCH1 staining. F. Merged image highlighting

strongly SMO+ cells in which PTCH1 is moderately elevated relative to adjacent SMO+ and SMO- cells.

Figure 3. Proliferation and caspase-3-mediated apoptosis as a function of genotype at 10 weeks of age. Each marker is shown at the top of the column to which it applies. Genotype of the mouse from which the gland was derived is shown to the left of the row to which it applies. Arrows highlight stained cells or regions of epithelium expressing the marker. A. BrdU and Ki67 (inset) staining, in wild type. B. Cleaved caspase-3 staining showing rare apoptotic cells. C. BrdU and Ki67 (inset) staining, in an *MMTV-SmoM2* gland. D. Cleaved caspase-3 staining showing a rare apoptotic cell. E-F. BrdU and cleaved caspase-3 staining, respectively, in a *ΔPtch1/+* gland displaying the characteristic ductal phenotype.

Figure 4. Dual immunofluorescence analysis of *MMTV-SmoM2* mice at 10 weeks of age. A. SMO/Ki67 showing no co-localization. B. SMO/ER showing no co-localization. C. ER/Ki67 showing low frequency co-localization, confirmed by BrdU/ER dual staining (inset). D. ER/CK6 showing high frequency co-localization. E. Duct showing ectopic CK6 expression, but no detectable SMO expression. (Inset) A region of high SMO expression lacking CK6 expression.

Figure 5. Effect of *MMTV-SmoM2* on mammosphere formation and regeneration of the mammary gland. A. Pairwise comparison of log-transformed mammosphere-formation efficiency values for five paired sets of primary epithelial cell preparations. *MMTV-SmoM2* cells showed a two-fold increase in mammosphere-forming efficiency relative to wild type cells in four of the five sample pairs. B. Statistical evaluation of mammosphere-forming efficiency including all five paired samples shown in A. C. Photomicrographs of representative mammospheres from *MMTV-SmoM2* and wild type mice. D. Photomicrographs of representative outgrowths of transplanted mammospheres derived from wild type

and *MMTV-SmoM2* mice. E. Limiting dilution transplantation analysis as a function of genotype. F. Photomicrographs of representative outgrowths from limiting dilution transplantations (100 cells).

Figure 6. PTCH1 and SMO protein expression in human breast cancer. Representative expression patterns are shown with total immunohistochemical score for the sample, with the proportion and intensity scores in parentheses. PTCH1 is readily detectable in normal breast epithelium and isolated stromal cells (A), but shows a relative loss in the epithelium in DCIS (B) and IBC (C) (P<.0001, Table 4). SMO expression is undetectable in normal breast (D), but is detectable in the cytoplasm in ~70% of DCIS (E) and ~30% of IBC (F) (P<.0001, Table4).

Figure 7. Dual immunofluorescence analysis of PTCH1-positive and SMO-positive human DCIS and IBC. A-F. PTCH1-Ki67 in DCIS and IBC. Representative staining patterns are shown that indicate extensive colocalization of PTCH1 with Ki67 in those samples expressing detectable PTCH1. G-J. SMO-Ki67 in DCIS and IBC. Representative staining patterns are shown that indicate rare colocalization of SMO with Ki67 in those samples expressing detectable SMO. K. Quantitative analysis of SMO-Ki67 colocalization in DCIS and IBC.

ACKNOWLEDGEMENTS

The authors are very grateful to Drs. Jeffrey Rosen, Gary Chamness, and Yi Li for critical comments on the manuscript. This work was supported by the National Institute of Health grants P01- CA30195 (M.T.L.), and P50-CA58183 (D.C.A.), and from the Department of Defense (IDEA) 17-00-1-0477 (M.T.L.).

Table 1. Antibodies used in our study.

Antibody name	Company	Clone/catalogue number	Concentration
Estrogen Receptor (ER)	Santa Cruz Biotechnology	MC-20	1:100
Progesterone Receptor (PR)	Santa Cruz Biotechnology	C-19	1:800
Ki67	Dako Cytomation	MIB-1	1:1000
Cleaved Caspase-3	Cell Signaling Technology	9661	1:25
Cytokeratin 6 (CK6)	Covance	PRB-169P	1:500
Patched-1 (PTCH1)	Santa Cruz Biotechnology	H-267	1:25
Smoothened (SMO)	Santa Cruz Biotechnology	N-19	1:50
Patched-1 (PTCH1)*	Santa Cruz Biotechnology	G-19	1:50
Smoothened (SMO)*	Santa Cruz Biotechnology	C-17	1:50
Donkey Anti-goat	Molecular Probes	-	1:200
Donkey Anti-rabbit	Molecular Probes	-	1:200

* Used on a subset of samples to confirm the expression patterns observed.

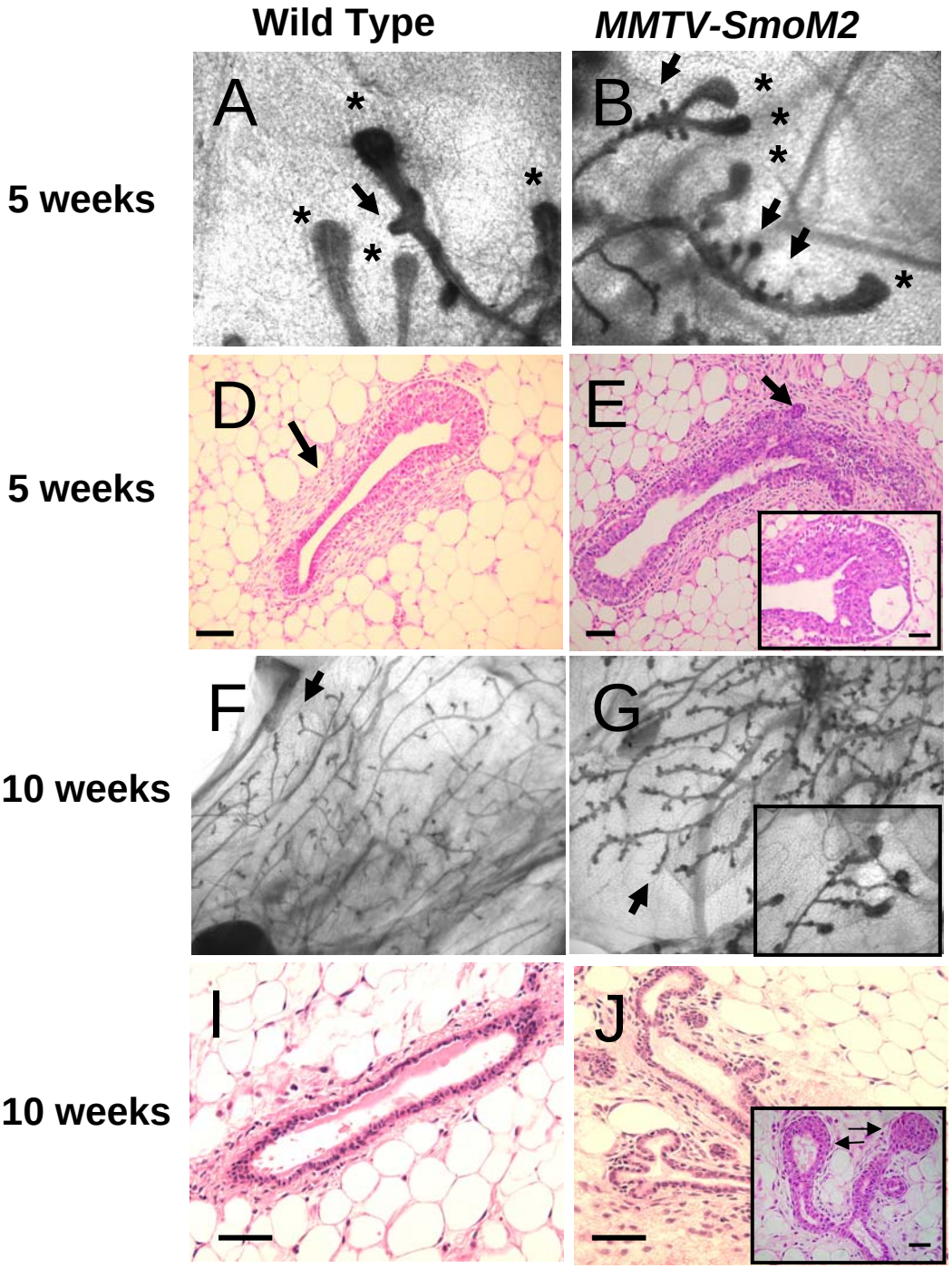
Wild Type
MMTV-SmoM2
5 weeks
5 weeks
10 weeks
10 weeks
A
B
D
E
F
G
I
J

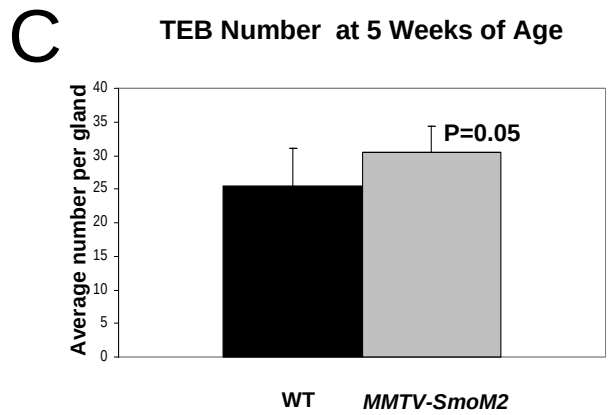
C
TEB Number at 5 Weeks of Age
Average number per gland
0
5
10
15
20
25
30
35
40
P=0.05
WT
MMTV-SmoM2

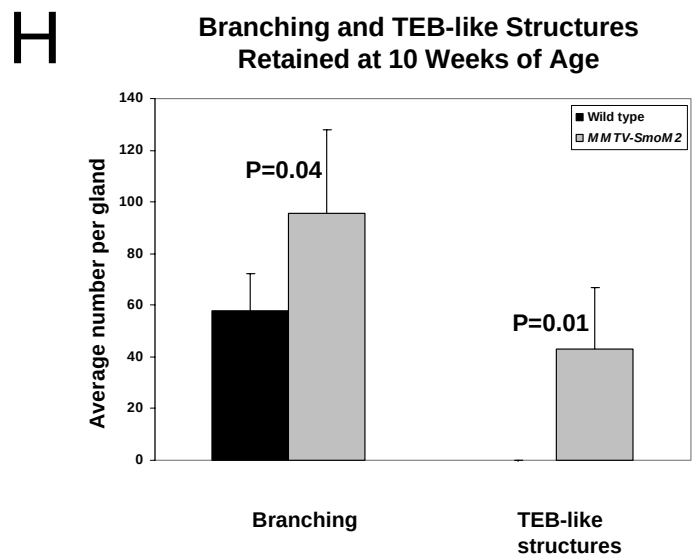
H
Branching and TEB-like Structures
Retained at 10 Weeks of Age
Average number per gland
0
20
40
60
80
100
120
140
Wild type
MMTV-SmoM2
P=0.04
P=0.01
Branching
TEB-like
structures

Figure 1

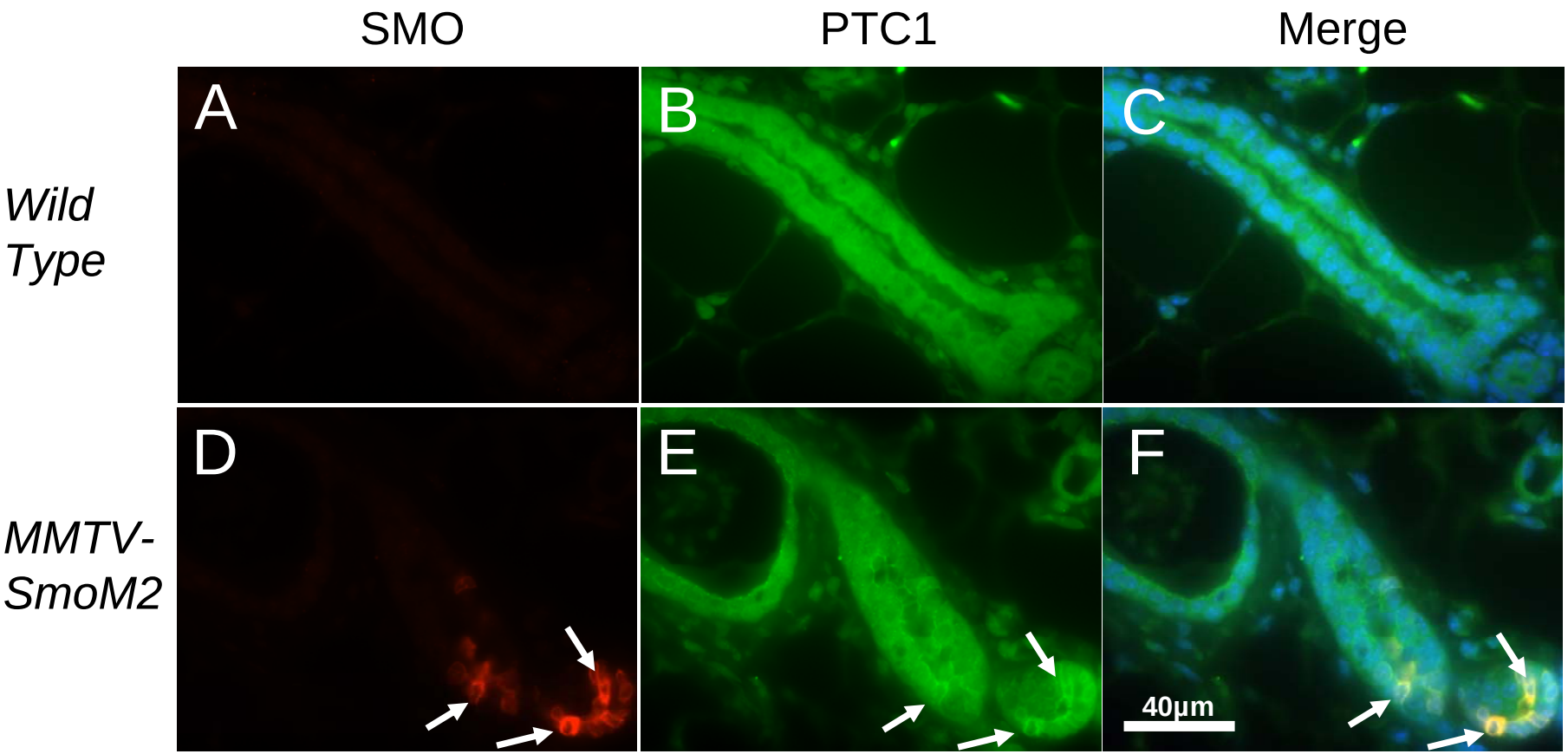

Figure 2

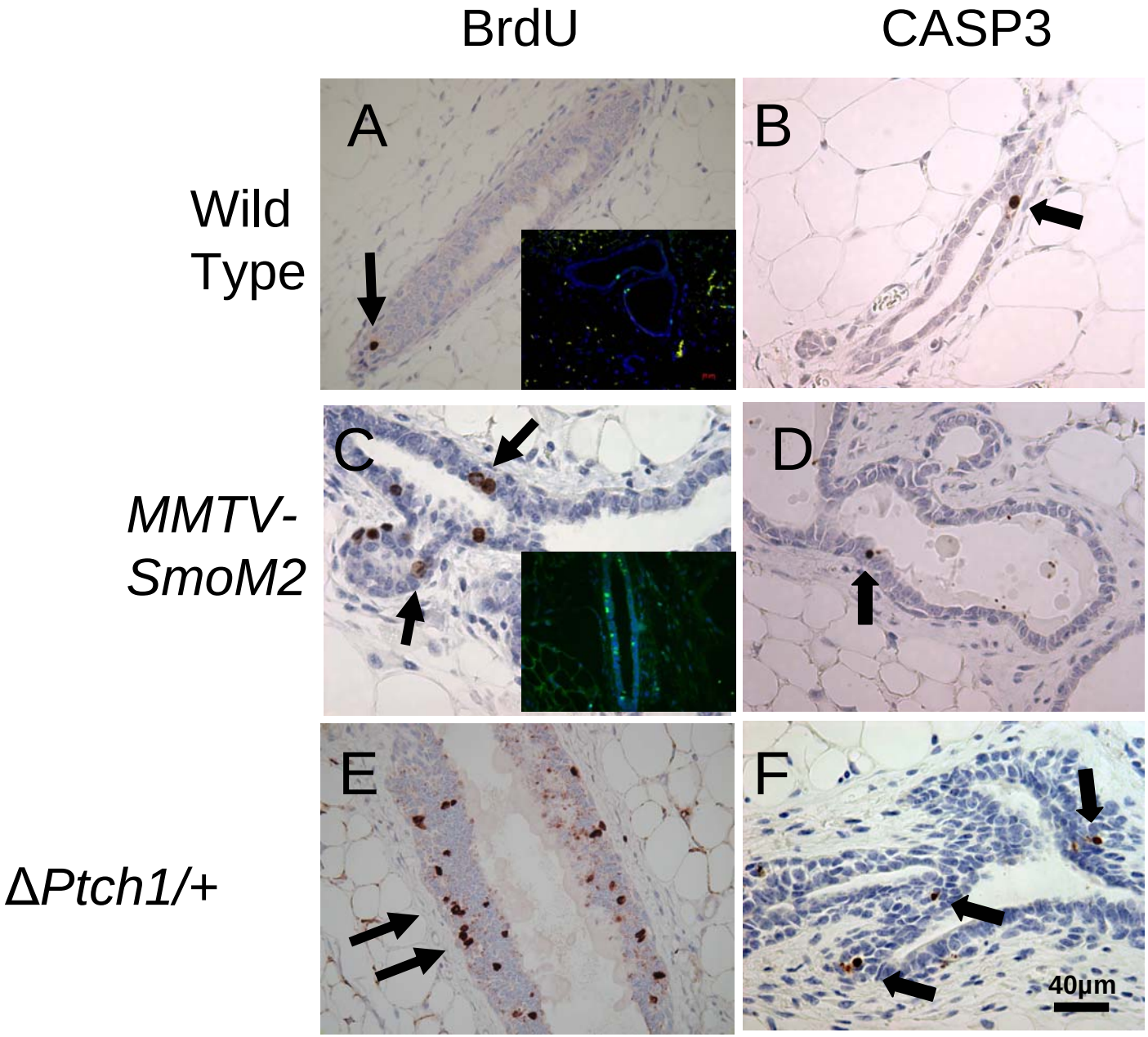

Figure 3

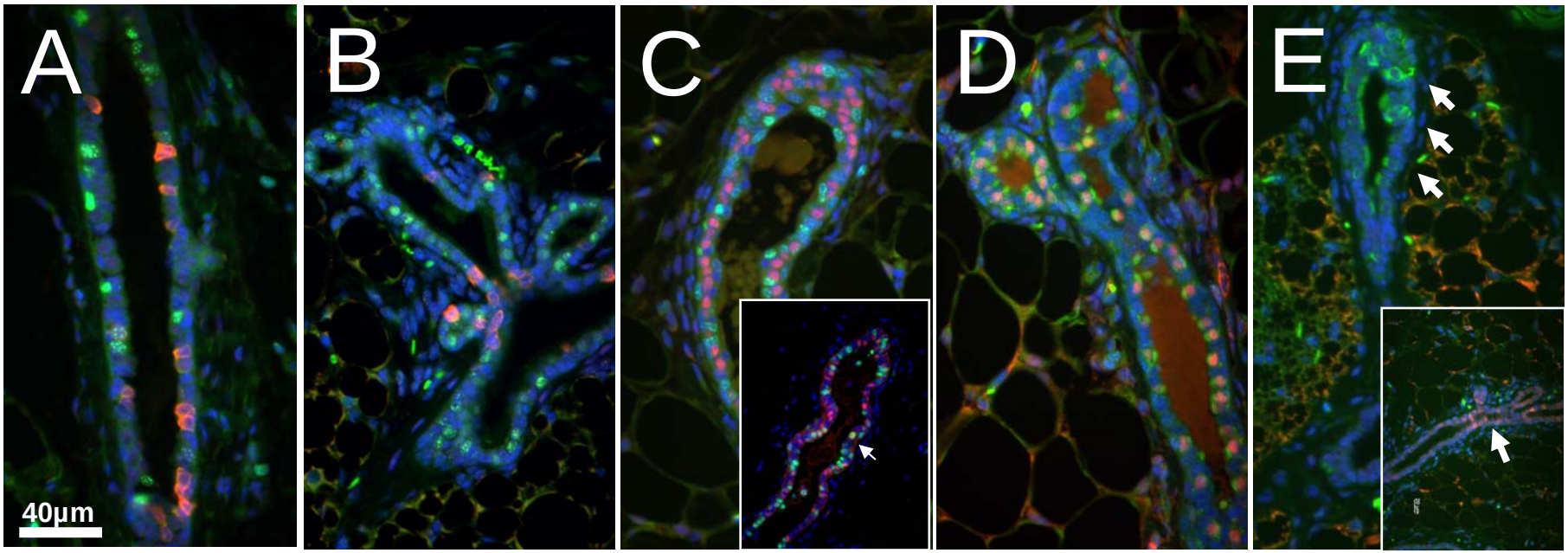

SMO+ Ki67+ = 0% SMO+ ER+ = 0% ER+ Ki67+ = 1.0% CK6+ER+ = 14.2% SMO+ CK6+ = 0%

Figure 4

A

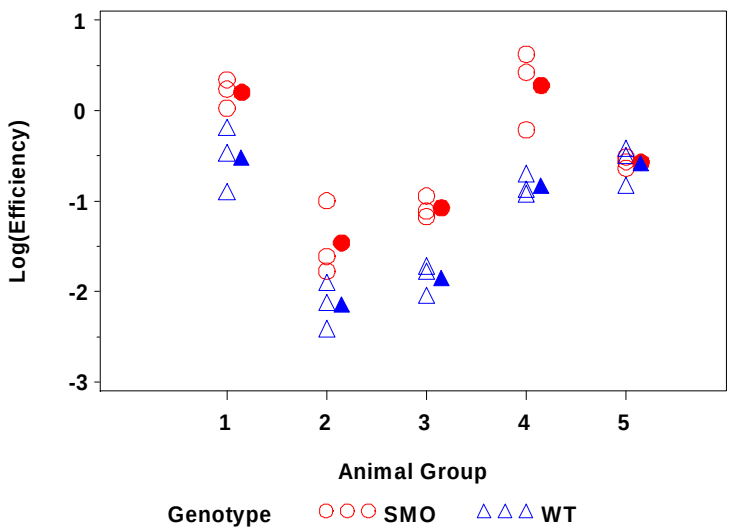

B

Table 2. Statistical Evaluation of Primary Mammosphere-forming Efficiency As a Function of Genotype.

T-Tests			
Difference	*DF*	*t Value*	*Pr > |t|*
SMO - WT	**4**	**3.67**	**0.0214**

C

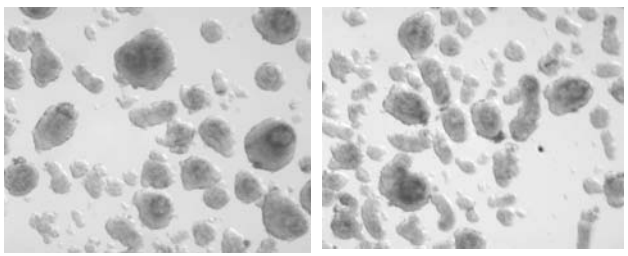

+/+ *MMTV-SmoM2*

D

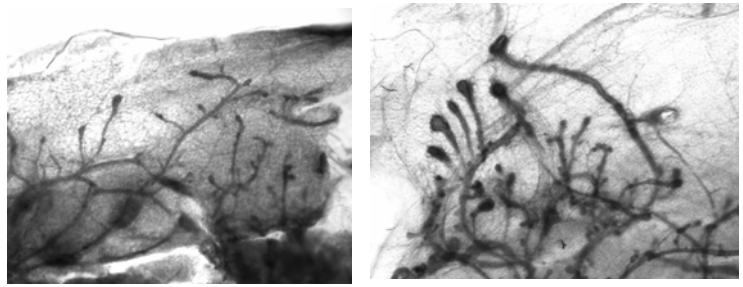

+/+ *MMTV-SmoM2*

E

Table 3. Limiting dilution transplantation analysis as a function of genotype.

	Genotype of epithelial cell donor			
	Wild type		*MMTV-SmoM2*	
Number of cells injected	Take rate	% fat pad filled	Take rate	% fat pad filled
1000	100% (4/4)	87.5 ±15.0	75% (3/4)	90 ±10.0
500	100% (10/10)	95 ±8.5	90% (9/10)	90 ±14.1
200	63% (5/8)	52 ±35.6	63% (5/8)	78 ±38.3
100	65% (11/17)	80 ±16.7	47% (8/17)	53.3 ±29.7
50	47% (7/15)	80 ±27.7	13% (2/15)	50 ±28.3
25	27% (4/15)	20 ±14.1	7% (1/15)	5 ±0.0
Regenerative stem cell frequency (upper and lower limits)	1/106 cells (1/72-1/156)		1/255 cells (1/166-1/390)	

F

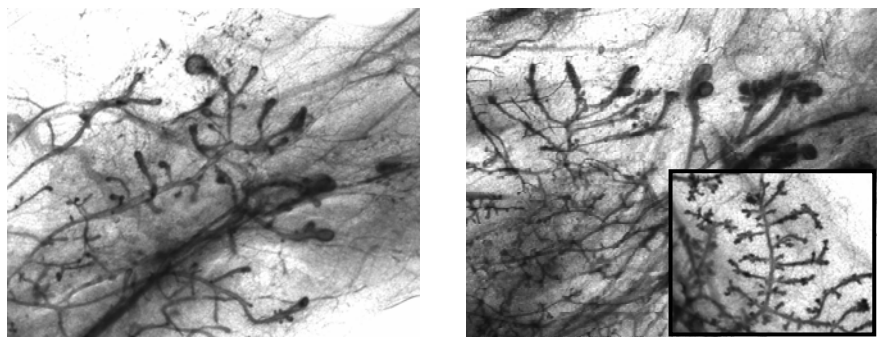

+/+ *MMTV-SmoM2*

Figure 5

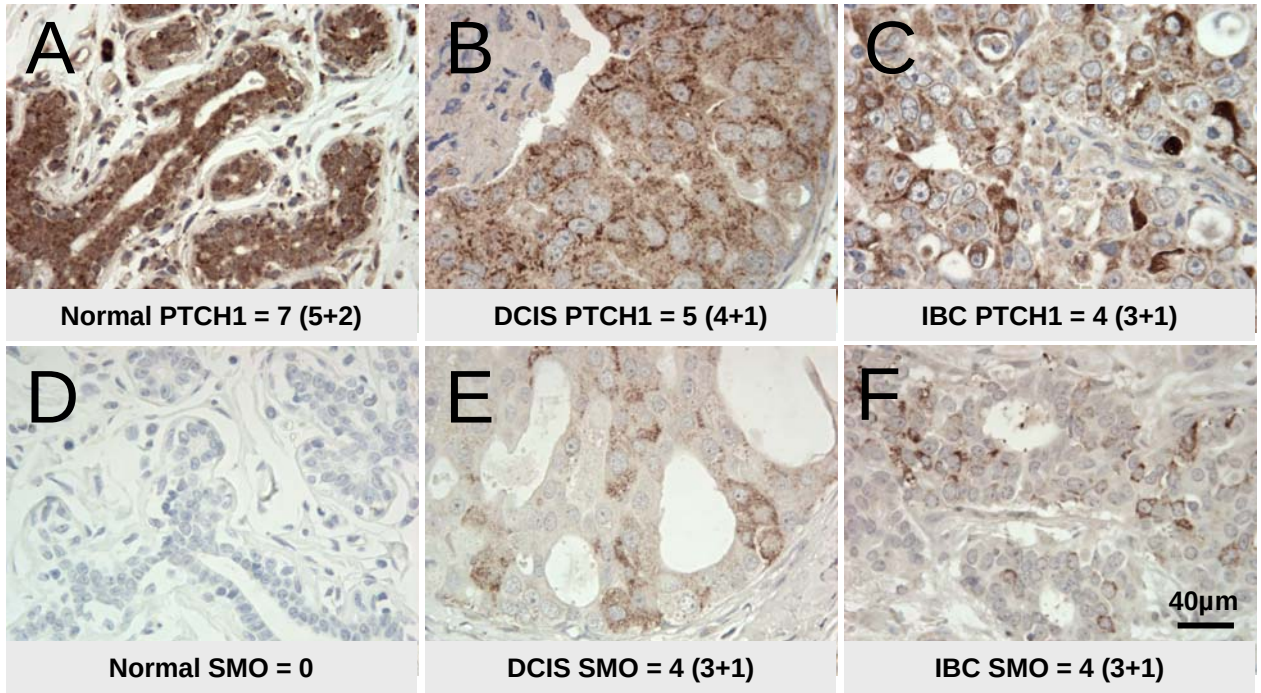

Table 4. Average total IHC scores for SMO and PTCH1 in clinical samples of human breast.

	SMO						PTCH1					
Tissue type	N	Mean	SD	Median	Min.	Max.	N	Mean	SD	Median	Min.	Max.
Normal (N)	7	0	0	0	0	0	17	6.76	0.56	7	5	7
DCIS (D)	167	2.57	1.51	3	0	5	172	5.50	1.55	6	0	8
IBC (I)	143	1.76	1.88	2	0	5	142	4.72	1.93	5	0	8

Wilcoxon rank-sum test for total scores

SMO	PTCH1
p=0.0003, N vs. D	p<0.0001, N vs. D
p=0.0163, N vs. I	p<0.0001, N vs. I
p=0.0003, D vs. I	p=0.0001, D vs. I

Figure 6

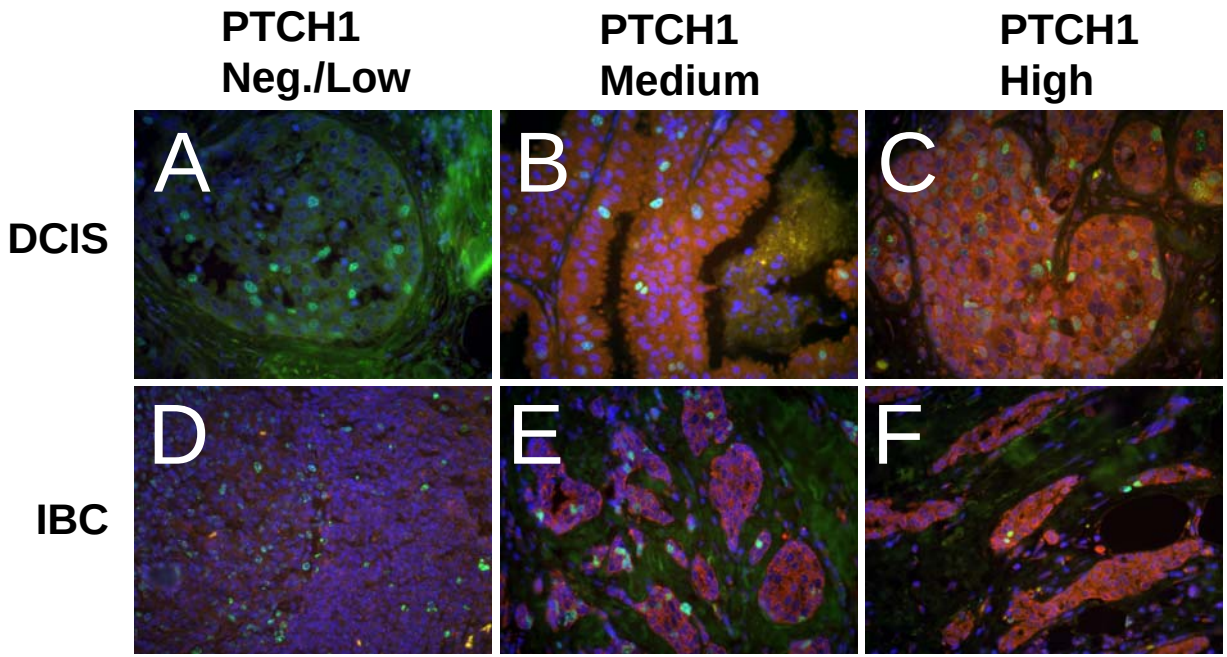
PTCH1
Neg./Low
PTCH1
Medium
PTCH1
High
DCIS
IBC
A
B
C
D
E
F

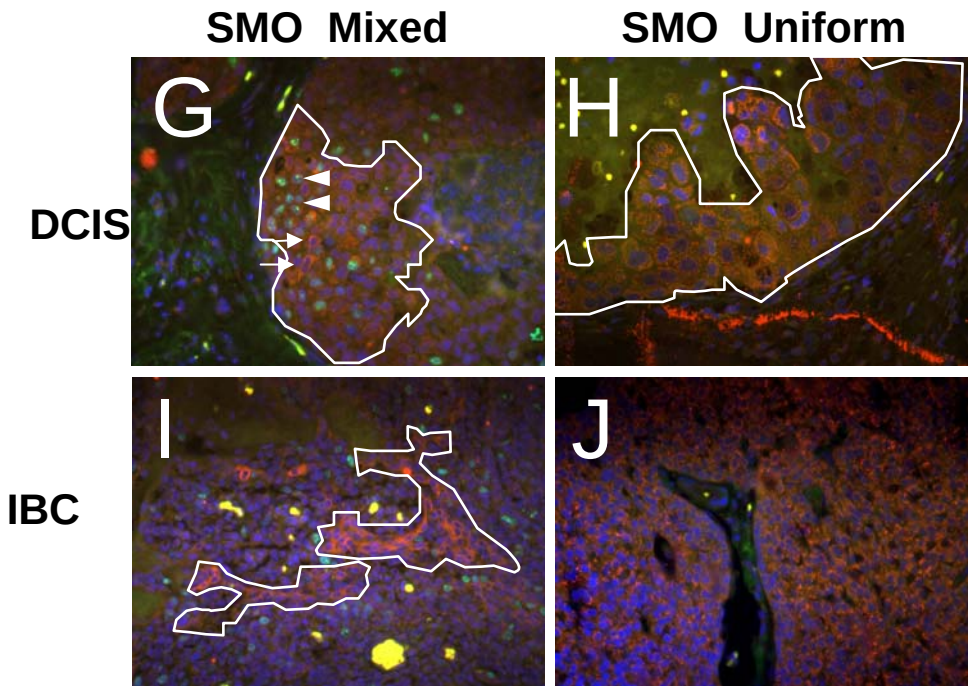
SMO Mixed
SMO Uniform
DCIS
IBC
G
H
I
J

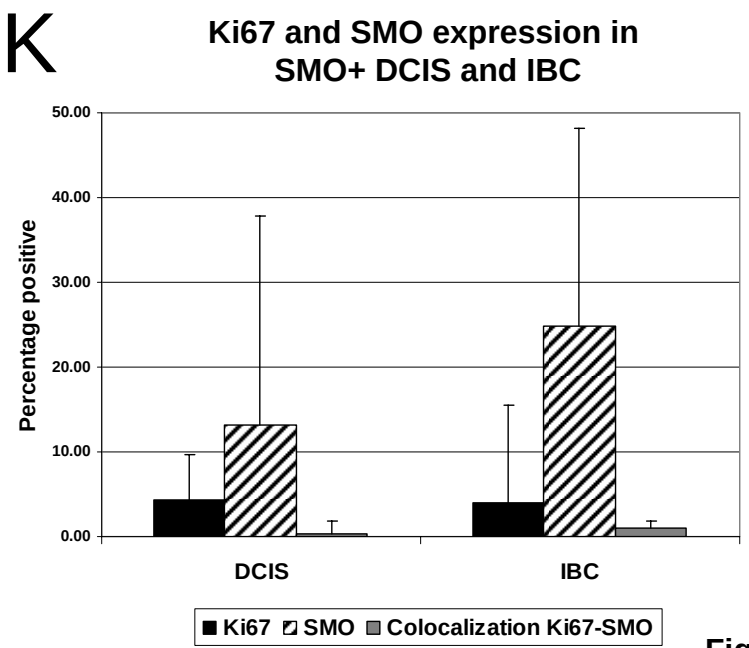
K
Ki67 and SMO expression in
SMO+ DCIS and IBC
Percentage positive
50.00
40.00
30.00
20.00
10.00
0.00
DCIS
IBC
Ki67
SMO
Colocalization Ki67-SMO

Figure 7